



ORIGINAL ARTICLE

A switchable-oxidative cellulose filter paper bearing immobilized Mn^(III)-salen complex for alcohol oxidation



Wei Long ^{a,b}, Andrei Sevbitov ^c, Saade Abdalkareem Jasim ^d, Olga Kravchenko ^e,
Moaed E. Al-Gazally ^f, Supat Chupradit ^g, Hamzah H. Kzar ^h, Milad Kazemnejadi ^{i,*}

^a College of chemistry, Guangdong University of Petrochemical Technology, Maoming 525000, PR China

^b Guangdong Provincial Key Laboratory of Petrochemical Pollution Process and Control, Guangdong university of petrochemical technology, Maoming 525000, PR China

^c Department of Propaedeutics of Dental Diseases, Sechenov First Moscow State Medical University, Moscow, Russia

^d Department of Medical Laboratory Techniques, Al-Maarif University College, Ramadi, Al-Anbar, Iraq

^e Kazan Federal University, Department of Legal Disciplines, Kazan Federal University, Russia

^f College of medicine, University of Al-Ameed, Karbala, Iraq

^g Department of Occupational Therapy, Faculty of Associated Medical Sciences, Chiang Mai University, Chiang Mai 50200, Thailand

^h Department of Chemistry, College of Veterinary Medicine, Al-Qasim Green University, Al-Qasim, Iraq

ⁱ Department of Chemistry, College of Sciences, Shiraz University, Shiraz 71946.84795, Iran

Received 2 April 2022; accepted 17 July 2022

Available online 22 July 2022

KEYWORDS

Cellulose filter paper;
Alcohol oxidation;
Schiff base and oximes;
Portable catalyst;
Environmentally protocol;
Catalytic filtration

Abstract Surface modifications of polysaccharide filter papers can alter their catalytic properties significantly. In particular, polysaccharides have gained increasing interest in the development of heterogeneous catalysts. This work introduces a new approach to the heterogeneous/ sustainable catalytic system preparation based on a catalytic filter paper modified by silylation followed by immobilization of a Mn(III)-salen complex as a novel “catalytic filtration” or “portable catalysis”. Oxidation of alcohols as well as direct conversion of alcohols to Schiff bases and oximes were performed by filtration and passing the reactants through the modified filter paper. Oxidation of benzyl alcohol in the presence of molecular oxygen and NaOCl, selectively leads to aldehydes and carboxylic acids, respectively. The direct conversion of alcohols to Schiff bases and oximes resulted in the formation of insoluble products on the filter paper. Another advantage of the modified filter paper was its stability and reusability for several times with preservation of the catalytic activity and swellability, which no shrinkage during consecutive wetting–drying cycles was observed. Also, a deep study was conducted over mechanism, reusability/stability, and control experiments of the

* Corresponding author.

E-mail addresses: Moaedalgazaly@gmail.com (M.E. Al-Gazally), miladkazmnejad@yahoo.com (M. Kazemnejadi).

Peer review under responsibility of King Saud University.



alcohol oxidation. This study gave new insights into the catalytic propensities of a cellulose filter paper *via* filtration of reactants.

© 2022 Published by Elsevier B.V. on behalf of King Saud University. This is an open access article under the CC BY-NC-ND license (<http://creativecommons.org/licenses/by-nc-nd/4.0/>).

1. Introduction

Polysaccharides are one of the most abundant natural polymers in nature, have the potential to replace petroleum-based polymers, which are difficult to decompose in paper coatings. Polysaccharide molecules with the numerous hydroxyl functional groups could be bind strongly with paper fibers *via* hydrogen bonds. Chemical modification of the polysaccharide papers can also constructively promote (or change) their hydrophobic/hydrophilic mechanical, and barrier properties and thus can further improve the desired properties of coated paper. Polysaccharides can also give paper additional functional properties by immobilizing nanoparticles, catalytic molecules, and functional fillers (e.g. antimicrobial chemicals or conductive particles), onto paper surface (Li, Wang, Jin, Huang, & Xiang, 2020; Lin, Huang, & Dufresne, 2012; Sheibani, et al., 2021).

Cellulose is a linear polysaccharide polymer bearing numerous glucose monosaccharide units. Cellulose is widely used in the preparation of various membranes and filter papers. Therefore, modifying a cellulose filter paper with catalytic organometallic molecules, so that the filtration method can be used for organic reactions, is an intelligent strategy that not only is environmentally friendly, but also addresses the problems associated with heterogeneous catalysts.

Although heterogeneous catalytic systems based on nanoparticles are recoverable and more environmentally friendly than their corresponding homogeneous systems, still have drawbacks such as agglomeration, loss in different cycles of re-use, and their toxicity on the environment (Fubini, Ghiazza, & Fenoglio, 2010; Niazi, & Gu, 2009). If it can be designed that the reaction catalyzed during filtration, it is possible to design an environmentally friendly system with easy work-up.

Cellulose filter paper has the advantage that its surface can be modified with organic molecules, and used as a heterogeneous catalyst in organic reactions as well as solid phase synthesis with clean work-up advantage (Nishikata, et al., 2014). Cellulose has been known as a suitable solid support in heterogeneous catalysts field. Due to the high ability to manipulate and modify a cellulose paper, it has attracted a lot of attention from scientists in various fields in order to achieve different goals (Nie, et al., 2020), that can be point to: (1) lipase-supported cellulose paper for transesterification reaction (Koga, Kitaoka, & Isogai, 2012), (2) Immobilized Pd NPs on surface of filter paper for sequential cross-coupling and hydrogenation reactions (Nishikata, et al., 2014), (3) Ag NPs-loaded filter paper as a catalytic system for nitro reduction, cascade reaction, and degradation of methyl orange (Mourya, Choudhary, Basak, Tripathi, & Guin, 2018), and (4) 3-mercapto-propanoic acid-modified cellulose filter as an adsorbent for the removal of arsenate from drinking water (Pramanik, Sarkar, & Bhattacharyay, 2019).

Paper-based electrodes (Yao, et al., 2017), Ag-doped cellulose filter paper as wound dressing agent (Haider, et al., 2018), Superhydrophobic paper with high self-cleaning properties (Musikavanhu, et al., 2019), and superhydrophobic cellulose paper for water drop energy harvesting (Nie, et al., 2020) are some other advances over manipulation of a cellulose filter paper and its application in various fields of sciences.

Despite numerous reports on the catalytic properties of a cellulose filter paper, none of them have used the filtration method because it is difficult to design a reproducible and reliable model accepted by chemists. For example, parameters such as filtration rate, ecofriendly conditions, and temperature must be controlled suitably, and the catalytic activity of the filter paper must be such that the reaction can take

place during filtration, because unlike routine laboratory reactions, the reaction mixture cannot be stirred. In addition, the filter paper modification and reaction conditions should not damage or degrade the quality of the filter paper.

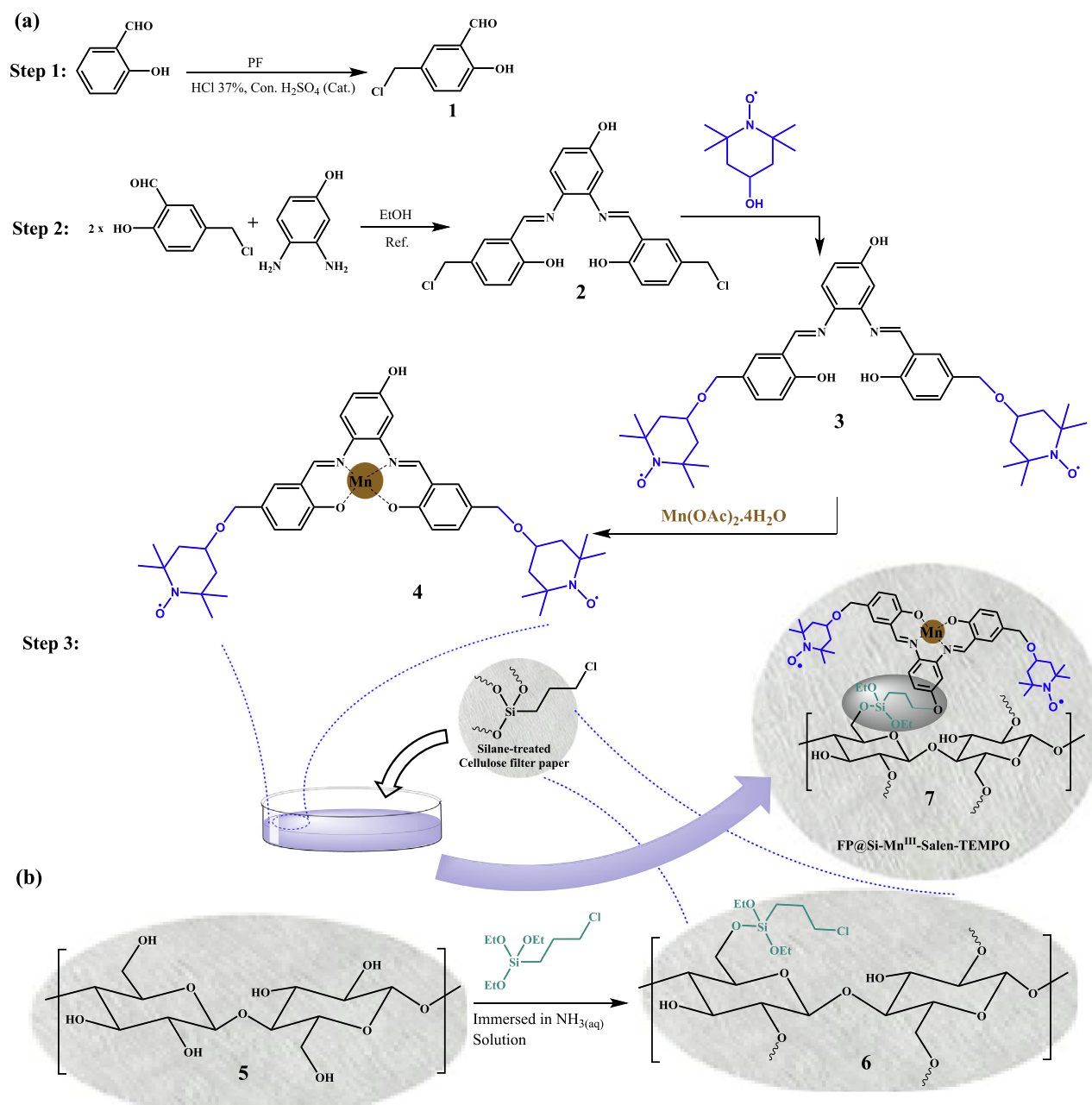
Another advantage of catalytic filter paper as a portable catalyst is its use in industry even by non-experts. Oxidation of alcohols is one of the reactions that requires such an innovation due to its widespread use in organic synthesis and industry. Alcohol oxidation is of great importance in the preparation of organic and pharmaceutical precursors as well as in the chemical and petrochemical industries, which due to its extent, it imports large volumes of waste from catalysts, toxic raw materials and oxidation byproducts into the environment (Deligeorgiev, et al., 2010). Given that the oxidation of alcohols requires high selectivity, because the oxidation of benzyl alcohols can potentially create ester, aldehyde and acid products, designing a suitable catalytic system for alcohol oxidation is important (Mahmoudi, Rostami, Kazemnejadi, & Hamah-Ameen, 2020). The lack of selectivity of the catalyst is not only unaffordable and introduces waste materials into the environment, but also makes it difficult to purify (work-up) the desired products (Kazemnejadi, Nikookar, Mohammadi, Shakeri, & Esmaeilpour, 2018). In addition to high selectivity, cost-effectiveness, repeatability and high stability in various conditions and being environmentally friendly are among the other factors that should be considered.

The studies have shown that the simultaneous presence of a transition metal complex along with an organic catalytic agent such as (2,2,6,6-tetramethylpiperidin-1-yl)oxyl (TEMPO) in a bi-functional catalytic system catalyst, provides a high synergistic effect for the oxidation of organic compounds in the presence of a suitable oxidant (Mahmoudi, Rostami, Kazemnejadi, & Hamah-Ameen, 2020). In addition, the presence of TEMPO not only increases the oxidation selectivity, but also has a synergistic effect on oxidation by proper interaction with the substrate (Hoover, Ryland, & Stahl, 2013; Ma, Mahmudov, Aliyeva, Gurbanov, & Pombeiro, 2020; Mahmoudi, Rostami, Kazemnejadi, & Hamah-Ameen, 2021; Nutting, Rafiee, & Stahl, 2018; Hu, & Kerton, 2012). In this work, in order to modify the cellulose filter paper for oxidation reactions, the Mn-salen complex was first functionalized by TEMPO groups and then immobilized on a pre-silylated filter paper. Silylation of cellulose paper was performed to immobilize Mn-salen complex *via* the covalent and reliable bond on cellulose fibrous (Scheme 1). Oxidation of alcohols to carbonyl as well as carboxylic acid groups was done selectively by filtration of the reactants through the catalytic bi-functional filter paper in the presence of molecular oxygen and NaOCl, respectively. In addition, direct conversion of oximes and imines from alcohols was also performed by the catalytic filter paper. Stability, recoverability of the filter paper, and the reaction mechanism were also studied. Scheme 2 shows the general schematic of the set-up reaction for the benzyl alcohol oxidation.

2. Experimental

2.1. Materials and methods

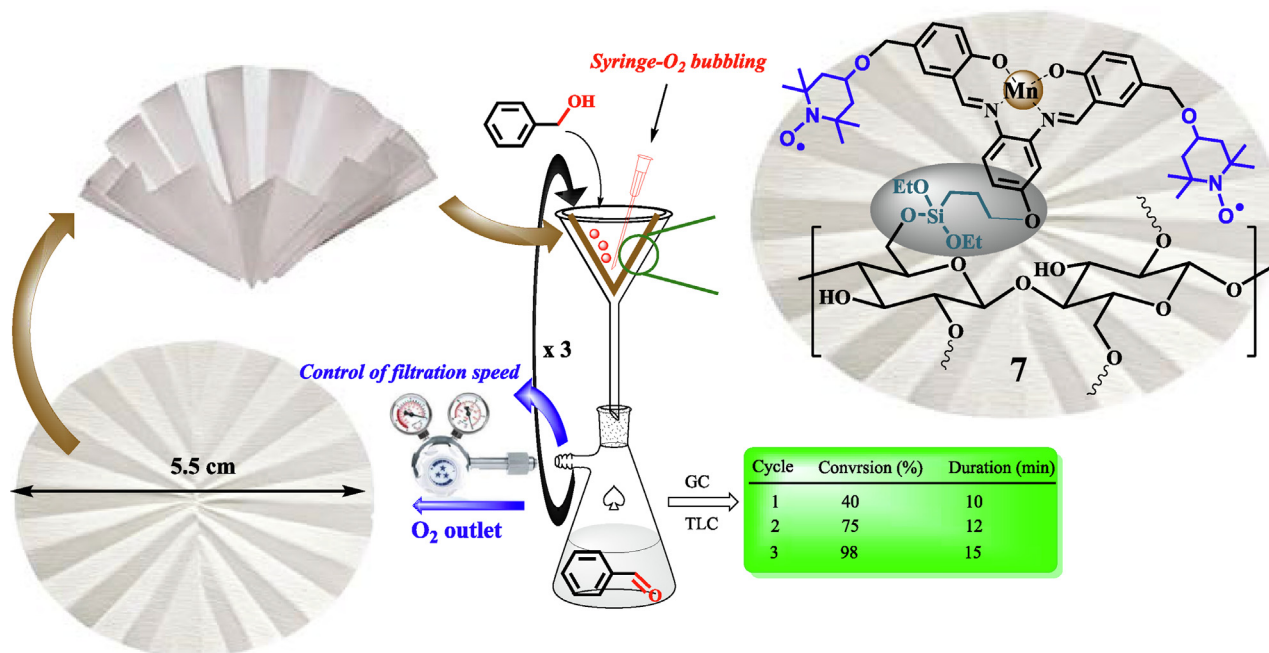
A circle folded Whatman cellulose filter paper (1201–320) grade 1 V, with a 0.2 mm thickness, 32 cm in diameter, 8–10 μm , 150 s/100 mL speed (Herzberg) with basic weight of 120 $\text{g}\cdot\text{m}^{-2}$ was purchased from Sigma in order to preparation of the catalytic filter paper. The reaction set up was equipped by a low pressure gas-inlet (0–1 bar) V-121 K091 R-21 regula-



Scheme 1 A schematic view for the preparation of (a) *N,N'*-(4-OH-phenylenebis(SA-5-TEMPO))-Mn^(III) complex (**4**) and FP@Si-Mn^(III)-Salen-TEMPO (**7**), and (b) silylation of the cellulose filter paper by 3-chloropropyltriethoxysilane (FP@Si-Cl).

tor (inlet connection W24,32), to control of filtration rate (contact time duration). Orbital Shaker, 10 mm Orbit from BTLabSystems was used for shaking. FTIR as well as ATR (in the case of filter papers) spectra were recorded on a JASCO FT/IR 4600 spectrophotometer. The NMR (¹H and ¹³C) spectra were recorded using a Bruker AVANCE III 300 MHz spectrometer in deuterated solvents including CDCl₃ and DMSO *d*₆. TMS was used as an internal standard. ICP analyses were performed on a NexION 2000B ICP Mass Spectrometer. Crystal structure of the samples was studied by X-ray diffraction (XRD) patterns of the samples on a Rigaku Smart-Lab X-ray diffractometer with Cu K α ($\lambda = 1.5418$ nm) radiation. Morphology of the samples were

studied by the field emission scanning electron microscopy (FE-SEM) technique using a Tescan MIRA3 apparatus. Elemental analysis of the samples was performed using EDX spectroscopy on a JEOL 7600F field emission scanning electron microscope, equipped with a spectrometer of energy dispersion of X-ray from Oxford Instruments. Experimental design for the statistical studies over the effective parameters on the benzyl alcohol oxidation as well as subsequent regression analyses of the experimental data were performed using a Design-Expert statistical software version 11, Stat-Ease Inc., Minneapolis, MN, USA. Gas chromatography analyses were performed on a YL 6100 gas chromatograph system (GC) with a CBP5 column (Shimadzu 30 m \times 0.32 mm \times 0.



Scheme 2 Representation of aerobic oxidation of benzyl alcohols using a portable FP@Si-Mn^{III}-Salen-TEMPO catalytic filter paper.

25 mm). The conversion and selectivity of the products was determined by GC software (Autochro-3000).

2.2. Synthesis of 2-hydroxy-5-(iodomethyl)benzaldehyde (SA-5-IM, 2)

2-Hydroxy-5-chloromethyl benzaldehyde (SA-5-CIM) was prepared according to the previously reported procedures (purple crystals, 97% isolated yield) (Mahmoudi, Rostami, Kazemnejadi, & Hamah-Ameen, 2020; Mahmoudi, Rostami, Kazemnejadi, & Hamah-Ameen, 2021; Nutting, Rafiee, & Stahl, 2018; Hu, & Kerton, 2012).

2.3. 2,2'-((1E,1'E)-((4-hydroxy-1,2-phenylene)bis(azanilylidene))bis(methanylylidene))bis(4-(chloromethyl)phenol) or N,N'-(4-OH-phenylenebis(SA-5-CIM)), 2

N,N'-(4-OH-phenylenebis(SA-5-CIM)) **2** was simply prepared with dissolution of SA-5-CIM (2.0 mmol) and 3,4-diaminophenol (1.0 mmol) in 20 mL dry EtOH under Ar atmosphere. The reaction was refluxed for 4 h with constant stirring. The resulting product was obtained by filtration of the cooled solution. The product was washed with cool EtOH and deionized water, then dried at 55 °C in a vacuum oven and isolated as a yellow solid.

Characterization data for *N,N'*-(4-OH-phenylenebis(SA-5-CIM)), **2**: Yellow powder; M.P. 144 °C; EDX analysis (% wt): C, 63.77; Cl: 16.92, O: 12.48, N, 6.83; Anal. Calcd. for C₂₂H₁₈ClN₂O₃: C, 61.55; H, 4.23%; N, 6.53%; Found: C, 61.59; H, 4.20 %, N, 6.54.

2.4. Synthesis of N,N'-(4-OH-phenylenebis(SA-5-TEMPO)), 3

For the preparation ionic compound **3**, *N,N'*-(4-OH-phenylenebis(SA-5-TEMPO)), as a ligand, *N,N'*-(4-OH-phenylenebis(SA-5-CIM)) (2.0 mmol) and 4.0 mmol of 4-OH-TEMPO were dissolved in dry ethanol. Then, triisopropylamine (4.0 mmol) was added to the mixture. The reaction was refluxed under Ar atmosphere for 3.0 h. Then, the resulting dark yellow solid was filtered after cooling the reaction mixture, and then washed with deionized water as well as 1.0 mL cool EtOH.

Characterization data for *N,N'*-(4-OH-phenylenebis(SA-5-TEMPO)), **3**: Pale yellow powder; M.P. 120 °C; EDX analysis (%wt): C, 71.80; O: 17.98, N, 10.22; Anal. Calcd. for C₄₀H₅₂N₄O₇: C, 68.55; H, 7.48%; N, 7.99%; Found: C, 68.50; H, 8.04 %, N, 7.99.

2.5. Synthesis of N,N'-(4-OH-phenylenebis(SA-5-TEMPO))-Mn^(III) complex, 4

Complexation of Mn ion to *N,N'*-(4-OH-phenylenebis(SA-5-TEMPO)) ligand was performed simply by dissolution of 2.0 mmol of ligand **3** and 1.0 mmol of Mn(OAc)₂·4H₂O to EtOH (20.0 mL) at room temperature. The reaction was stirred for 2.0 h and the resulting brown solid was filtered, washed with deionized water as well as cooled EtOH, then isolated as a stable brown powder at room temperature for the next step.

Note: Different synthetic routes was evaluated for the synthesis of 4 (Scheme S1), and the routes shown in Scheme 1 was chosen as the most promising and repeatable with the highest efficiency for the preparation of catalytic filter paper 7.

2.6. Silylation of cellulose filter paper

For the silylation of cellulose FP, two protocols could be used:

(1) Silylation of cellulose filter paper was inspired by the work of Chantereau *et al.* (Chantereau, *et al.*, 2019) in water. The plain filter paper was soaked in a basicified (with NH₃ solution, pH = 9.0) aqueous solution of (3-chloropropyl)triethoxysilane (340 mM). The set up was shacked for 24 h at room temperature to complete adsorption/ deposition of 3-chloropropyltriethoxysilane (CPTES) on the FP. Then, the paper was freeze-dried for 24 h and stored in a desiccator with P₂O₅ before use.

(2) In the second protocol, a simple chemical vapor deposition was served according to a previously reported protocol with some modifications (Jankauskaitė, Balčiūnaitienė, Alexandrova, Buškuvienė, & Žukienė, 2020). This method was used to expose cellulose filter paper (CFP) to the CPTES vapor in the absence of any catalyst at an elevated temperature. 25 mL of CPTES was added to a closed chamber bearing an open vessel holding the CPTES. Then, a plain CFP was placed on a porous filter paper and the temperature was adjusted to 215 °C. The test was repeated at three different time intervals of 2, 6, 8, 12 h. Cellulose filter papers treated by vapor deposition were marked as SiCFPvap.

2.7. Preparation of N,N'-(4-OH-phenylenebis(SA-5-TEMPO))-Mn^(III) complex, (4)-embedded filter paper (FP@Si-Mn^{III}-Salen-TEMPO)

In first, N,N'-(4-OH-phenylenebis(SA-5-TEMPO))-Mn^(III) complex, **4** (200 mg) was added to a 6 cm diameter glassy petri dish containing 15 mL of ethanolic ammonia solution. The presence of ammonia also helps to neutralize the acid produced during CPTES coupling to the hydroxyl groups in the cellulose. Then, the silylated cellulose filter paper with 5.5 cm in diameter was slowly inserted into the petri dish. In order to immobilize the manganese complex **4** into the filter paper covalently, the petri dish was shacked for 48 h at room temperature. Then the filter paper was washed with deionized water and ethanol to remove any salt, contaminate or un-coupled complex **4** on the paper. The FP@Si-Mn^{III}-Salen-TEMPO filter paper was dried and stored in a vacuum desiccator containing P₂O₅ as a desiccant and dehydrating agent.

2.8. General procedure for FP@Si-Mn^{III}-Salen-TEMPO catalyzed oxidation of alcohol to aldehydes

The filtration set-up was provided by a glass funnel placed on a vacuum Erlenmeyer flask, then the folded modified catalytic filter paper was placed on the funnel. The flask was equipped with a low pressure N₂ inlet (0.3 bar) using a V-121 K091 R-21 regulator (inlet connection W24,32) to control the filtration rate. Then, a mixture of benzyl alcohol (10.0 mmol) in 5.0 mmol of EtOH: H₂O (2:1) was poured on the filter paper in one step, so that the entire surface of the filter paper was covered by the reaction mixture (the reaction mixture rose to near the edge of the filter paper). Using a O₂ source, molecular oxygen was bubbled with rate of 1.0 mL/mL into the solution placed on the filter paper. The tip of the syringe was placed at the bottom of the filter paper into the solution and the system was completely sealed. The filtration rate was controlled using

a valve regulator installed in the Erlenmeyer outlet to provide the necessary and appropriate time for the reactants to interact with the filter paper surface. The filtration was performed at room temperature. At each filtration, the reaction progress was monitored by TLC and GC. Finally, the filter paper was washed with 10 mL of hot absolute ethanol three times.

The reaction time was accurately calculated by the stopwatch and only during the contact of the reactants with the filter paper (filtration time only). For each filtration, the time was calculated immediately after pouring the reactants on the filter paper and the time was stopped after the filtration was completed. After each filtration (each run), the selectivity and conversion was determined by GC analysis; Because, there is no catalyst species in the filtrate. The next cycle was repeated in the same way. Due to the constant pressure in Erlenmeyer, the filtration follows a constant mean time. The total measured times were reported in Tables 1-3.

The resulting mixture of each reaction was directly injected to GC instrument. By having the pure products as well as injecting them into the device, the selectivity and conversion of the products was determined by GC software (Autochro-3000).

Selectivity of the products were measured qualitatively by gas chromatography. For each experiment, the resulting mixture (0.2 μL) was injected to GC instrument then the selectivity of the products was calculated by the following equation (Mahmoudi, Rostami, Kazemnejadi, & Hamah-Ameen, 2020):

$$\text{Conversion (mol\%)} = \frac{(\text{initial mol\%}) - (\text{final mol\%})}{\text{initial mol\%}} \times 100$$

$$\text{Benzaldehyde selectivity} = \frac{\text{GC peak area of Benzaldehyde}}{\text{GC peak area of all products}} \times 100$$

2.9. General procedure for FP@Si-Mn^{III}-Salen-TEMPO catalyzed oxidation of alcohol to carboxylic acids

The same procedure as for the oxidation of benzyl alcohol to aldehyde (section 2.8) was used for the direct oxidation of alcohol to carboxylic acid, except that instead of O₂ bubbling, 25 mmol NaOCl as an oxidant was used, which was initially added to the mixture in order to filtration.

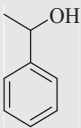
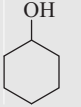
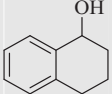
2.10. General procedure for FP@Si-Mn^{III}-Salen-TEMPO catalyzed direct preparation of imines and oximes from alcohols

The direct conversion of alcohols to imines (or oximes) was performed as same procedure as used for the oxidation of benzyl alcohol to benzaldehyde, except that a mixture of 1.0 mmol benzyl alcohol, 1.2 mmol primary amine (or NH₂OH·HCl for the preparation of oximes) dissolved in 5 mL of EtOH:H₂O (2:1) was used for the filtration. Imine (or oxime) products formed on both filter papers and Erlenmeyer's inside. In this way, after 3 consecutive filtrations, the mixture collected in Erlenmeyer was stirred at room temperature by adding a magnet for a few minutes. Finally, the reaction mixture was filtered again, then the imine (or oxime) product was collected on filter paper, then purified by recrystallization from ethanol.

Table 1 Oxidation of alcohols to carbonyl compounds catalyzed by FP@Si-Mn^{III}-Salen-TEMPO *via* filtration.

| Entry | Alcohols | Product | | | | | |
|-----------------|----------|---------------------------------|-----------------------------|-----------------------|-----------------------------|------------------------------|-----------------------|
| | | Carbonyl (route 1) ^a | | | Acid (route 2) ^b | | |
| | | Product | Time (min)/NOF ^c | Con. ^d (%) | Product | Time (min) /NOF ^c | Con. ^d (%) |
| 1 | | 9a | 37/3 | 98 | 10a | 37/3 | 95 |
| 2 | | 9b | 37/3 | 92 | 10b | 37/3 | 82 |
| 3 | | 9c | 37/3 | 90 | 10c | 37/3 | 80 |
| 4 | | 9d | 37/3 | 96 | 10d | 37/3 | 86 |
| 5 | | 9e | 37/3 | 98 | 10e | 37/3 | 95 |
| 6 | | 9f | 37/3 | 82 | 10f | 37/3 | 80 |
| 7 | | 9g | 37/3 | 85 | 10g | 37/3 | 80 |
| 8 | | 9h | 37/3 | 86 | 10h | 37/3 | 82 |
| 9 | | 9i | 37/3 | 96 | 10i | 37/3 | 85 |
| 10 | | 9j | 37/3 | 80 | 10j | 37/3 | 72 |
| 11 | | 9k | 54/4 | 80 | 10k | 37/3 | 75 |
| 12 ^c | | 9l | 75/5 | 75 | 10l | 54/4 | 80 |

Table 1 (continued)

| Entry | Alcohols | Product | | | | | |
|-------|---|---------------------------------|-----------------------------|-----------------------|-----------------------------|------------------------------|-----------------------|
| | | Carbonyl (route 1) ^a | | | Acid (route 2) ^b | | |
| | | Product | Time (min)/NOF ^c | Con. ^d (%) | Product | Time (min) /NOF ^c | Con. ^d (%) |
| 13 |  | 9 m | 100/6 | 80 | 10 m | – | – |
| 14 |  | 9 n | 75/5 | N.R. | 10 n | – | – |
| 15 |  | 9 o | 100/6 | 65 | 10 o | – | – |

^a Reaction conditions: Benzyl alcohol (10.0 mmol), EtOH: H₂O (2:1, v/v, 5.0 mL), O₂ bubbling (1.0 mL/min), catalytic filter paper 7 (placed on a glass funnel, containing 2.0 mmol Mn/95 cm²), room temperature for 3 consecutive re-filtration of the residue. Selectivity = 97–99%. ^b Reaction conditions: NaOCl (25 mmol). Selectivity = 94%. ^c Number of filtration. ^d GC yield. ^e Therephthaldehyde and therephthlic acid were the major products for route 1 and route 2 respectively.

2.11. Other set-ups

In order to benefit from the highest catalytic activity of the filter paper, in addition to the filtering protocol, three other protocols of (1) cutting the filter paper and using it in the reaction mixture (like a heterogeneous catalyst), (2) suspending the filter paper components inside the reaction mixture (Nishikata, et al., 2014), and (3) a filtration mode equipped with a O₂ flow (instead of O₂ bubbling) were also studied and compared.

(1) In the first set-up, the filter paper was cut into several 1 cm square pieces and added to the reaction medium as a heterogeneous catalyst. The reaction was stirred in the presence of a magnet bar and its progression was studied by GC or TLC analyses. In this method, the filter papers were separated from the reaction medium by forceps in the end of the reaction and in order to achieve the maximum efficiency, the filter paper pieces were placed in a plate containing 15 mL of pure ethanol for 5 h and the plate was shaken for 1 h. The resulting solution was then added to the reaction mixture to determine the conversion percentage.

(2) In this case, the filter paper with a diameter of 5.5 cm in accordance with the method presented by Nishikata et al. (Nishikata, et al., 2014) was kept inside the reaction mixture by a clamp, with the difference that in order to make a logical comparison with the other two methods (because Mn loading is depends on the surface area of the catalyst), a sheet of the catalytic filter paper 7, divided into 8 equal cone-shaped parts with a rim size of 2.75 cm and held suspended by a clamp inside the reaction mixture. The reaction was stirred by a magnetic stirrer and the progress of the reaction was monitored by GC or TLC. As in set-up 1, the filter paper pieces were shaken in 15 mL of pure ethanol to achieve the highest efficiency (to ensure that the filter paper contained no products) and the resulting solution was added to the reaction mixture.

(3) In addition, in another set-up, the reaction reactor was designed to use an O₂ gas flow (at the same rate) instead of bubbling it. For this purpose, the oxidation of benzyl alcohol

was performed and purified in exactly the same way as the main filtration procedure.

3. Results and discussion

3.1. Characterization investigations over Mn(III)-salen complex

Characterization studies were performed in two phases on compound 4 as well as on filter paper 7 step by step and after confirming formation of the desired products in each step, the synthesis continued and the compound was used for the next step. Figs. S1,S3-S10 shows the results of FTIR and NMR (¹H & ¹³C) analyses for 1–4. It is also worth mentioning that based on previously published articles, different synthetic pathways were evaluated to prepare compound 4 (ESI, Scheme S1) and the synthetic pathway shown in the Scheme 1 was the most optimal and reproducible pathway in order to prepare compound 4.

3.2. Characterization investigations over the FP@Si-Mn^{III}-Salen-TEMPO

The catalytic filter paper 7 was also characterized by different analyzes at each stage including ATR-IR, XRD, EDX, XPS, TGA, and FE-SEM analyses, and after confirmation, the synthesis steps were continued. Filter papers 6, 7 as well as unmodified (pristine) filter paper (5) were characterized by ATR-IR technique (ESI, Fig. S2).

In order to study the spectral changes resulting from the modifications made on the filter paper, the pristine filter paper was completely characterized by similar analyzes. ATR-IR spectrum of the cellulose filter paper (ESI, Fig. S2) showed three characteristic peaks at 1021 cm⁻¹, 1085 cm⁻¹, and 1156 cm⁻¹ related to the stretching vibrations of C-O-C glycoside bond, C-O-H anti-symmetric in plane, and C-O-C asymmetric bridge, respectively (Hinterstoisser, & Salmén, 2000; Hospodarova, Singovszka, & Stevulova, 2018).

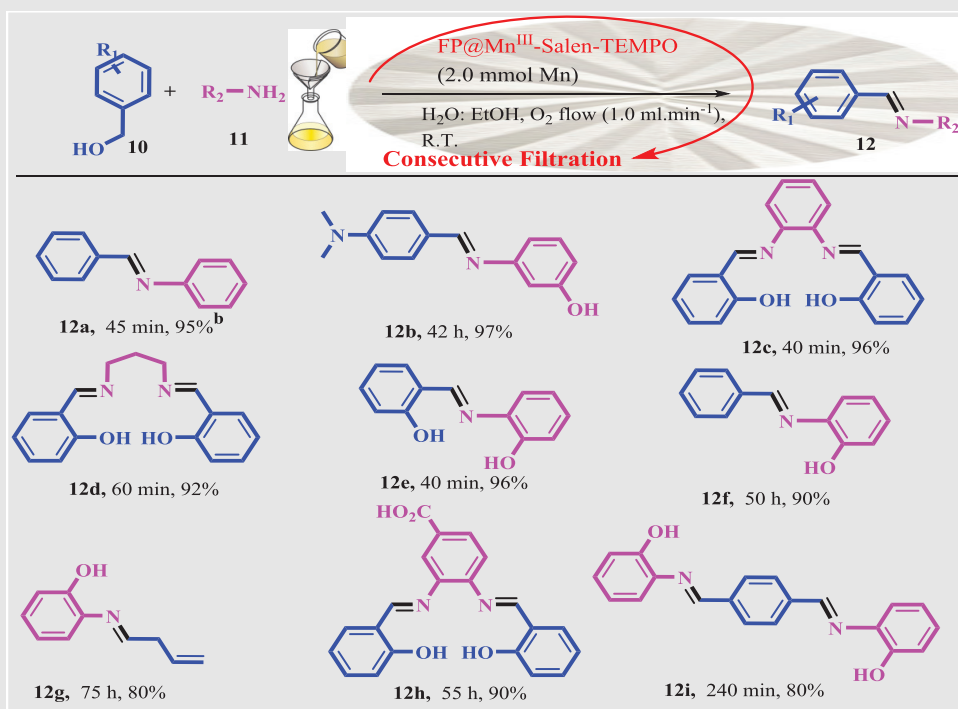
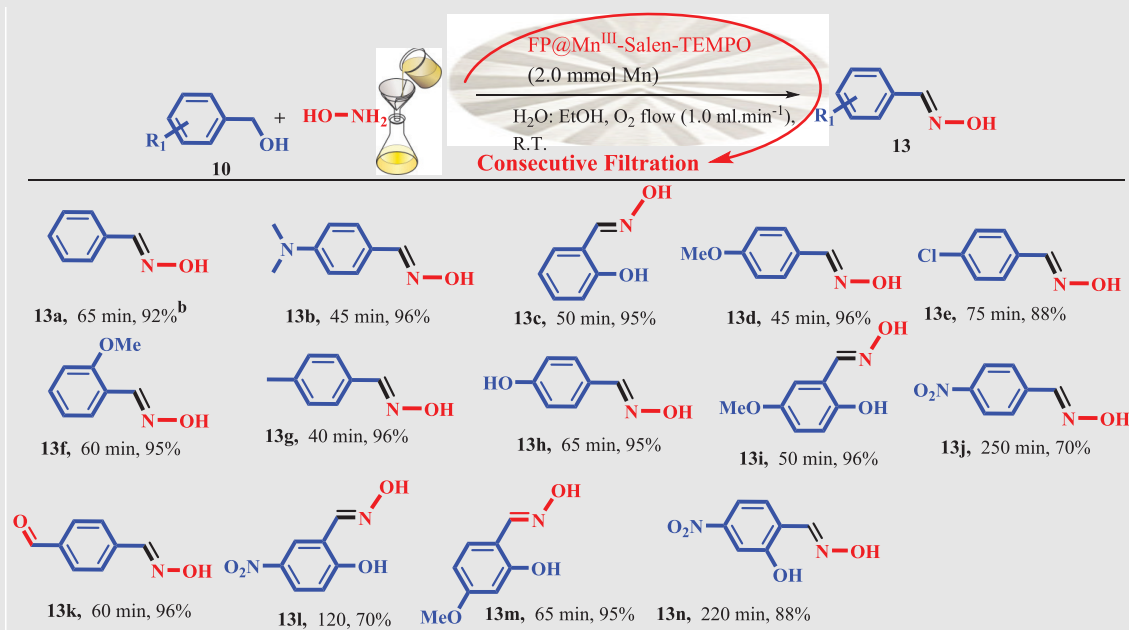
Table 2 Fe₃O₄@SiO₂@Im[Cl]Mn(III)-complex catalyzed one-pot preparation of imine by oxidation of alcohol *via* filtration^a.^bIsolated yield.^a Reaction conditions: Benzyl alcohol (1.0 mmol), amine (1.2 mmol), EtOH: H₂O (2:1, v/v, 5.0 mL), O₂ bubbling (1.0 mL min), catalytic filter paper 7 (placed on a glass funnel, containing 2.0 mmol Mn/95 cm²), room temperature for 3 consecutive re-filtration of the residue. After the filtrations, the filtrate was stirred at room temperature for appropriate time.

Fig. S11 shows other characterization analyses for the pristine cellulose. XRD analysis of the unmodified and were shown in Figure S11-a, wherein the presence of peaks appearing at $2\theta = 14.1^\circ, 16.2^\circ, 22.2^\circ$ indicates the crystalline structure of the cellulose filter paper in full accordance with the literature (Figure S11-a) (Kamal, Khan, Haider, Alghamdi, & Asiri, 2017). The presence of only C (51.36 wt%) and O (48.64 wt %) elements in the filter paper in the EDX spectrum, indicates the purity and the absence of any impurities in the filter paper (Figure S11-b). The elemental composition was further confirmed by XPS (overall survey) analysis that confirmed again the presence of C, O elements (Figure S11-c) as well as the purity of the paper. Thermal decomposition of the unmodified filter paper takes place in one step, starting at 280 °C and ending with a steep slope at 410 °C, that was in agreement with the literature (Fig. S11-d) (Youssef, Kamel, El-Sakhawy, & El Samahy, 2012). As shown in Figure S11-e, cellulose fibrous in the plain filter paper have a diameter of about 17 μm .

In this paper, inspired by previously reported methods (Chantereau, et al. 2019; Jankauskaitė, Balčiūnaitienė, Alexandrova, Buškuvienė, & Žukienė, 2020), cellulose filter paper was successfully silylated with a high weight percentage of Si. Silylation of a filter paper was performed using both aqueous solution and chemical vapor deposition (CVD) methods and studied by EDX (mean of 5 points) as well as ICP analyses. ICP analysis was studied after preparation of ash from the filter paper at 500 °C. According to the results, Si %wt in the silylated filter paper by aqueous solution and CVD was equal to 14.68 %wt and 12.90 %wt from ICP anal-

ysis, respectively (Table S1). As shown in Table S1, the results of ICP and EDX were so close to each other that confirms the accuracy of the results and the subsequent successful silylation. Despite the similarity of the results of both CVD and immersion method (solution), the filter paper was silylated by immersion method due to advantages such as room temperature, simple work up, cost-effectiveness, etc. In CVD method, different exposure times of 2, 6, 8, 12 h were studied, which the highest CPTES loading occurred at 6 h and the loading rate did not increase significantly after that. The loading rates at the exposure times of 2, 6, 8, 12 h were equal to 7.14, 12.77, 12.76 and 12.80 %wt, respectively. It seems that after 6 h the surface becomes saturated and cannot be loaded more by CPTES. The presence of strong vibrations at 780 cm^{-1} and 1073 cm^{-1} were related to the symmetric and asymmetric Si-O-Si stretching vibrations, respectively (Chantereau, et al., 2019), which confirms the successful silylation of the filter paper (ESI, Fig. S2-b). The results were in line with the EDX analyses of the silylated filter paper. Successful immobilization of the silica groups was also confirmed in the X-ray diffraction pattern of the silylated filter paper by the presence of an amorphous peak at $2\theta = 4^\circ$. In addition, by comparing the X-ray diffraction pattern of pristine cellulose (Figure S11-a), the deviation of the peaks from the crystalline state also confirms the presence of amorphous silica groups on cellulose fibers (Fig. 1-a). According to the results of EDX analysis, the presence of 11.36 %wt Si in the silylated filter paper, not only confirms the success of the silylation process, but also the high amount of loading allows the optimal immobilization of the

Table 3 Fe₃O₄@SiO₂@Im[Cl]Mn(III)-complex catalyzed one-pot preparation of oxime by oxidation of alcohol *via* filtration^a.^bIsolated yield.

^a Reaction conditions: Benzyl alcohol (1.0 mmol), NH₂OH·HCl (1.2 mmol), EtOH: H₂O (2:1, v/v, 5.0 mL), O₂ bubbling (1.0 mL min), catalytic filter paper 7 (placed on a glass funnel, containing 2.0 mmol Mn/95 cm²), room temperature for 3 consecutive re-filtration of the residue. After the filtrations, the filtrate was stirred at room temperature for appropriate time.

Mn complex with a high loading percentage. The presence of the Cl-related peaks at the 2.6 eV (Cl K α) and 2.8 eV (Cl K β) binding energies are another confirmation of the successful immobilization of the CPTES on the filter paper (Fig. 1-b). XPS analysis of the silylated filter paper also confirmed the obtained results by EDX analyses (Fig. 1-c). TGA analysis in agreement with ATR-IR and XRD analyzes confirmed the successful covalent immobilization of the silica groups (Fig. 1-d). Silylation of the filter paper causes a significant increase in the thermal stability of the filter paper than the pristine filter paper. As shown in Fig. 1-d, the thermal decomposition was performed with a gentle slope and at the end, the residual weight was about 35%, which by abstraction from the remaining weight of the pristine filter paper in the previous step, the residual weight of 28% could be attributed to the remaining silica groups. This thermal behavior was similar to the thermal behavior of the previously reported crosslinked polymers (Uhl, et al., 2001). The presence of silica groups on cellulose fibrous causes Si-O-Si bonds formation and consequently reduces the mobility of cellulose fibrous and provides high thermal stability for the filter paper. As shown in Fig. 1-e, the diameter of the cellulose fibrous reaches about 22 μm after silylation (Fig. 1-e), in agreement with its XRD pattern that the presence of the silyl groups was demonstrated by the amorphous peak at $2\theta = 4^\circ$. In addition, the density of cellulose fibrous was slightly increased and the amount and diameter of porosities were reduced. Also, the plate-shaped areas (non-fibrous areas) represent the cross-linked cellulose fibrous resulting through silica groups.

The immobilization of complex 4 on the silylated filter paper was confirmed by the presence of the characteristic peaks related to C = N as well as strong vibrations of C = C (corresponding to benzene rings) at 1650 cm⁻¹ and 1457 cm⁻¹, respectively in the ATR-IR spectrum of FP@Si-Mn^{III}-Salen-TEMPO filter paper (ESI, Fig. S2-c). In the next step, in order to ensure the successful immobilization of complex 4 on the filter paper, the filter paper was placed on a glass funnel and washed 3 times, each time with 10 mL of absolute ethanol, and the remaining solution was analyzed by ICP-MS analysis (Zhao, Liu, Shi, Shi, & Shen, 2019). Obviously, no trace of any metal (including Mn and Si leaching) was observed in the results, which reflects the covalent and stable immobilization of complex 4 through the ether bond according to what is shown in Scheme 1 and in agreement with its corresponding ATR-IR spectrum. The X-ray diffraction pattern of the filter paper 7 confirmed the presence of two phases, including silicate groups and the Mn complex. According to the X-ray diffraction pattern of filter paper 7, the amorphous peak appearing at $2\theta = 4.5^\circ$ was corresponds to the amorphous structure of silicate groups on the cellulose fibrous (Fig. 2-a) (Jankauskaitė, Balčiūnaitienė, Alexandrova, Buškuvienė, & Žukienė, 2020). Immobilization of amorphous silica groups as well as Mn-salen complex caused the X-ray diffraction pattern for cellulose to be somewhat deviated from the crystalline state, which confirms the successful immobilization of silica and Mn-salen complex compounds, in agreement with the ATR-IR spectrum.

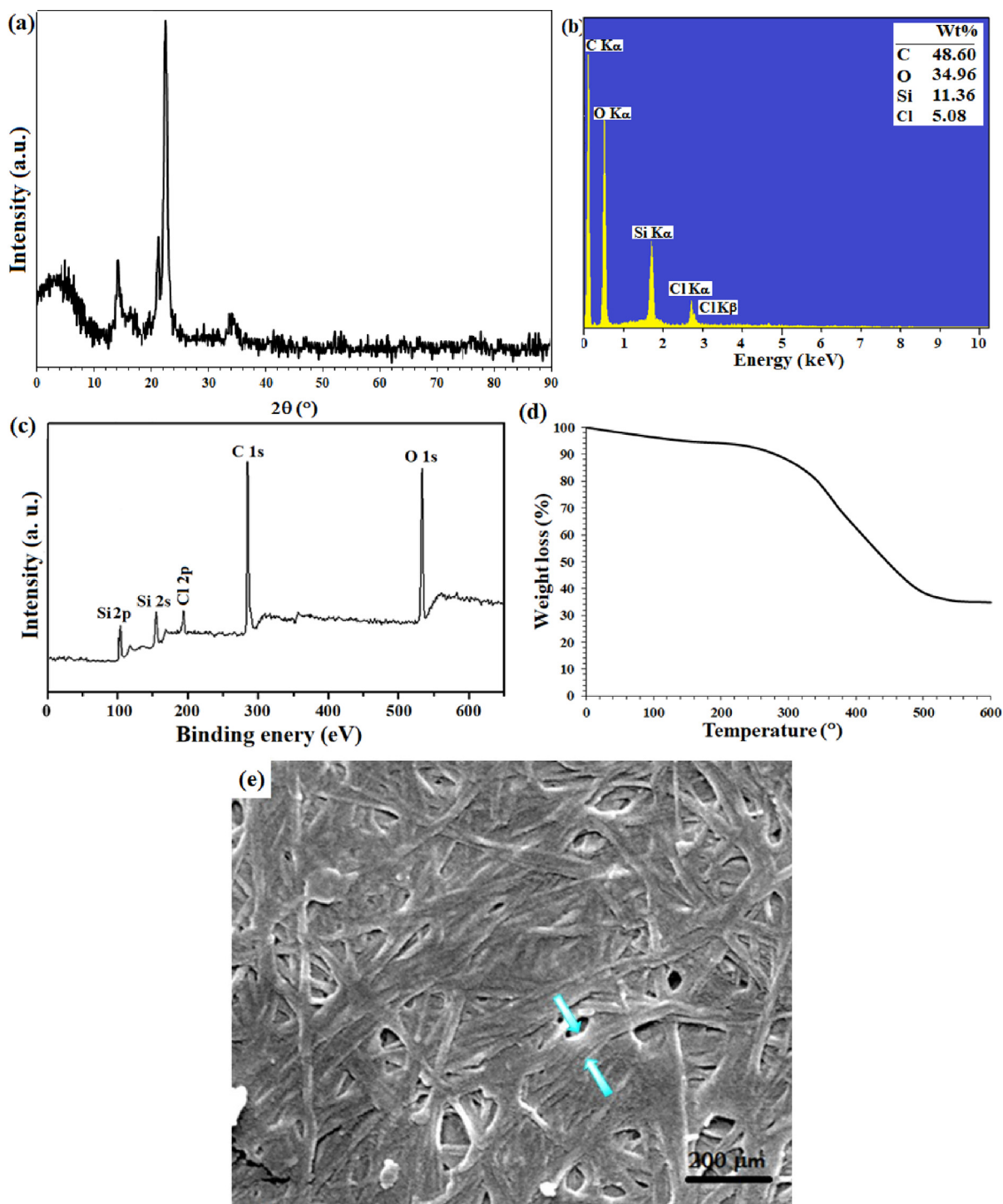


Fig. 1 (a) XRD pattern, (b) EDX spectrum, (c) XPS overall survey analysis, (d) TGA analysis, and (e) FE-SEM image of the silylated filter paper.

The loading contents of Si and Mn were measured on the prepared filter papers **6** and **7**, respectively (Scheme 1) by ICP-MS analysis of the resulting ash from the filter paper. For this purpose, the modified filter paper was placed in a crucible (0.9 g) and then calcinated in an oven at 500 °C under air atmosphere. At the same time, an unmodified (pristine) filter paper was calcinated as a control under exactly the same conditions. Based on the results of ICP-MS analysis, the modified filter paper **7** contains 2.45 wt% Mn and 13.92 wt% Si. The

elemental composition of filter papers **6** (silylated) and **7** (catalytic filter paper) was also studied by EDX analysis. According to the EDX spectrum of of FP@Si-Mn^{III}-Salen-TEMPO filter paper, the identification of Mn and N elements at binding energies of (5.9 Mn K α and 6.2 Mn K β eV) and 0.3 eV, respectively, confirms the successful immobilization of the complex on the filter paper. Complete removal of peaks related to Cl binding energies indicates that all silica groups were involved in the immobilization of the Mn^{III}-salen complex and also

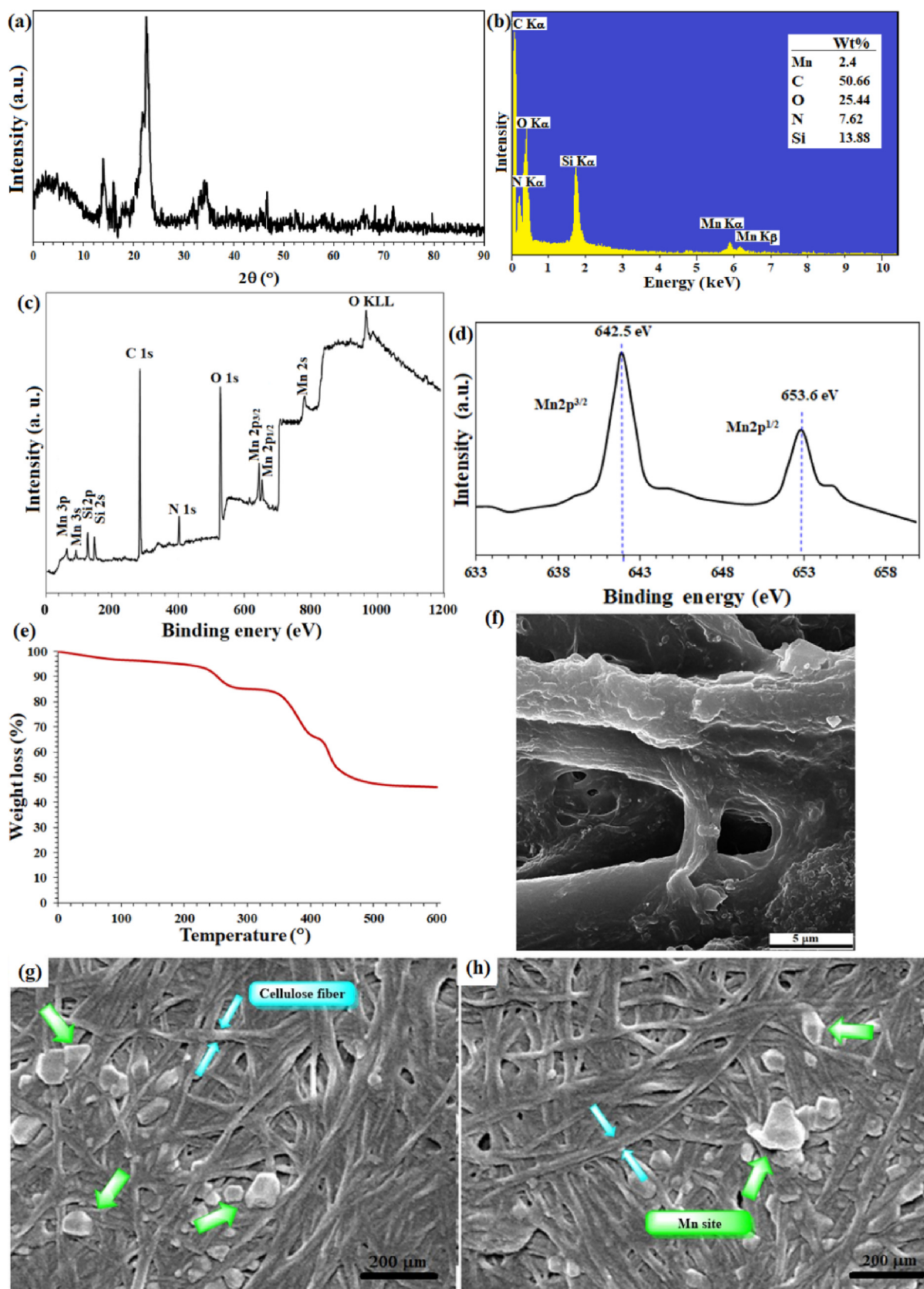


Fig. 2 (a) XRD pattern, (b) EDX spectrum, (c) XPS overall survey analysis, (d) high resolution XPS-Mn 2p (normalized, energy corrected) analysis, (e) TGA analysis, and (e),(f),(g) FE-SEM image of FP@Si-Mn^{III}-Salen-TEMPO filter paper.

the immobilization of the complex occurred through covalent bonding according to what is shown in [Scheme 1](#). ([Fig. 2-b](#)). XPS analysis of FP@Si-Mn^{III}-Salen-TEMPO filter papers also confirmed the successful immobilization of the Mn^{III}-salen complex **4** on the filter paper in full agreement with the EDX results ([Fig. 2-b](#)). XPS overall survey analysis of filter paper **7** also confirmed the presence of all elements including Mn as well as the absence of Cl in agreement with the EDX analysis ([Fig. 2-c](#)). High resolution XPS analysis was performed on filter paper **7** to determine the oxidation state of the coordinated Mn in structure of the salen ligand (immobilized on the filter paper). As shown in [Fig. 2-d](#), the binding energies for Mn 2p_{3/2} and Mn 2p_{1/2} have appeared at 642.5 eV and 653.6 eV, respectively, with an energy band gap of 11.1 eV, that was exactly belongs to Mn⁺³ ([Tang, Jiang, Liu, Wang, Sun, 2014; Biesinger, et al., 2011](#)). The study on the thermal behavior of FP@Si-Mn^{III}-Salen-TEMPO filter paper clearly confirmed the functionalization of the filter paper with the Mn^{III}-salen complex. Immobilization of the Mn^{III}-salen complex due to the presence of C = N bonds has given more stability to the filter paper ([Fig. 2-e](#)). Schiff base compounds have a special place in heat-resistant polymers ([Baran, Saçak, 2017](#)), therefore, the immobilization of the Mn-salen complex (with coordinated Mn ions) has resulted in greater thermal stability in the catalytic filter paper. The presence of 3 peaks in the thermal decomposition of FP@Si-Mn^{III}-Salen-TEMPO was evidence of the presence of multiple immobilized phases on the surface of filter paper, which was in agreement with previous analyzes. As shown in [Fig. 2-e](#), two peaks appearing at 270 °C (corresponding to 13% weight loss) and at 360 °C (corresponding to 3% weight loss) could be attributed to the decomposition of the imidazolium moieties (according to their weight loss percentages) and the Mn^{III}-salen ligand decomposition, respectively. The final peak at 426 °C was also related to the residual decomposition of silica-functionalized cellulose fibrous. SEM images from the plain, silylated and modified filter paper with Mn^{III}-salen complex **4** also show the preparation of filter paper **7** in accordance with other analyzes. Immobilization of Mn^{III}-salen complex **4** on the silylated cellulose fibrous results in clearer spots (indicated by green arrows) on the FE-SEM image of FP@Si-Mn^{III}-Salen-TEMPO, indicating the successful immobilization of complex **4** on cellulose fibrous ([Fig. 2-f,g,h](#)). Cellulose fibers are also marked with a blue arrow.

Given that the oxidation reactions will be done by the filtration set up, the amount of swelling of the filter paper by the reaction solvent is a critical parameter. Accordingly, the most suitable solvent is that preferably has the highest swelling rate and also provides satisfactory efficiency for the coupling reactions. [Table S2](#) shows the results of swelling measurements for plain, silylated, and FP@Si-Mn^{III}-Salen-TEMPO filter papers. Silylation of the surface of the filter paper significantly increased the swelling, which was higher for protic solvents than for polar ones. The results are completely consistent with the thermal behavior of the silylated filter paper, in which the possible cross-linking between the cellulose fibrous results in a rigid structure and greater stability than in the plain filter paper. The results of TGA also showed that the surface silylation significantly increases the thermal resistance of the filter paper. But with the immobilization of the Mn^{III}-Salen complex, the swelling rate for all solvents decreased. As shown in [Table S2](#), the amount of swelling in polar solvents such as

DMSO and DMF has decreased compared to this amount in silylated filter paper; However, for protic solvents, the reduction in swelling was slightly lower than for the silylated filter paper. The highest swelling was measured for FP@Si-Mn^{III}-Salen-TEMPO in aqueous solvent: ethanol equal to 14.6 mL/g.

3.3. Screening of reaction parameters

In order to more comprehensively investigate the reaction parameters and find the optimal point, the optimization reactions were designed by Design Expert software and the tests were designed on the reaction of the benzyl alcohol oxidation to benzaldehyde (model reaction) (ESI, [Figs. S12–S14](#), [Tables S3-S5](#)). [Tables S6 to S10](#) show the results and data of some tests. Based on these analyzes, the %conversion of the benzyl alcohol depends on all 3 parameters of the O₂ bubbling rate, the amount of Mn loading on the surface of the paper, and the reaction temperature (ESI, [Figs. S12–S14](#), [Tables S3-S5](#)).

In the first step, the loading of Mn-salen complex **4** on 95 cm² surface (on the filter paper with a diameter of 5.5 cm) was studied in the oxidation of benzyl alcohol to benzaldehyde. For this purpose, different ethanolic concentrations of Mn-salen complex including 0.3, 0.7, 1.2, 2.5 mmol were prepared and immobilized on the filter paper according to the procedure presented in the experimental section. [Table S6](#) shows the effect of different loadings of Mn-salen complex on the filter paper. According to the ICP results of the prepared filter paper, the covalent immobilization of the Mn-salen complex has an average efficiency of 80%. The results showed that in 2.0 mmol of Mn loading, the highest possible conversion for the benzyl alcohol oxidation to benzaldehyde was equal to 98% during three consecutive filtrations (37 min) ([Table S6](#), entry 4). Increasing the Mn loading to 2.5 mmol had no effect on the %conversion of benzyl alcohol, but at 2.5 mmol of Mn, the reaction time increased slightly and the efficiency decreased slightly. On the other hand, at lower amounts of 1.0 and 0.5 mmol of Mn, the %conversions were reduced to 70% and 30%, respectively. Significantly, a significant increase in the reaction time was consistent with an increase in Mn loading on the filter paper. As the loading of the Mn-salen complex increases, the porosity of the filter paper decreases and the reactants become more difficult to filtrate. Although this reduction in porosity leads to an increase in the contact time between the filter paper surface and the reactants, this increase in contact time does not lead to a significant increase in %conversion. On the other hand, polar-polar interaction between polar groups of silica (in addition to polar OH groups in cellulose) in the filter paper and polar solvent EtOH:H₂O, increases the reaction time, as observed by different solvents.

The oxidation of benzyl alcohol to benzaldehyde was studied as a model reaction to evaluate the effective parameters including oxidant, paper surface area, reaction temperature, solvent type, and the amount of Mn loading on the filter paper. First, the effect of solvent and oxidant type were studied. With the exception of molecular oxygen which bubbled as a syringe into the reaction mixture, other oxidants were added directly to the reaction mixture. [Table S7](#) shows the effect of different oxidants on the %conversion of benzyl alcohol. As shown in [Table S7](#), most oxidants gave high conversion rates, but there was a difference in selectivity. Due to the possibility of forma-

tion of various products in the oxidation of benzyl alcohol (Kazemnejadi, Nikookar, Mohammadi, Shakeri, & Esmailpour, 2018), the selectivity of the method is of great importance. Molecular oxygen produced the highest selectivity of 98% for benzaldehyde, next air and m-CPBA give 96% selectivity for 37 min (3 consecutive filtrations). Due to the fact that air also contains about 20% of molecular oxygen, the low efficiency provided by air indicates the dependence of the reaction to molecular oxygen. This phenomenon was in agreement with the catalytic oxidation systems based on TEMPO and a coordinated transition metal (Ma, et al., 2019; Chandra, Jonas, & Fernandes, 2018; Sharma, Buckley, & Asefa, 2008; Lu, et al., 2008). On the other hand, the oxidation of benzyl alcohol in the presence of NaOCl was quite selectively converted to benzoic acid. In addition, H₂O₂ and NaIO₄ oxidants also selectively (with less %conversion) oxidized benzyl alcohol to benzoic acid. It should be noted that according to studies on the stability of the filter paper in acidic, alkaline and oxidizing environments (that will be discussed in the next sections), the catalytic filter paper in oxidizing environments such as H₂O₂ and NaOCl was completely stable and no leaching or shrinkage in the filter paper during consecutive wetting–drying cycles occur. Therefore, as will be studied below, direct oxidation of benzyl alcohols to carboxylic acid will be performed in the presence of NaOCl as an oxidant.

The rate of oxygen bubbling as an oxidizing agent was also studied. According to the results, a rate of 1 mL/min was sufficient to achieve the highest efficiency for the reaction (Table S8, entry 3). The benzyl alcohol conversion decreased at lower O₂ rates and also in the absence of air, the benzyl alcohol conversion was 60%. Significantly, there was a decrease in selectivity at higher molecular O₂ flow rates. At higher oxygen flows, the surface appears to be saturated, and by interfering with the oxidation process, it not only reduces the benzyl alcohol conversion, but also reduces selectivity by formation of various by-products.

The solvent was studied as the next effective parameter. Due to the fact that the reaction will take place on the surface of the catalyst, so the diffusion is a determining factor for the oxidation. It seems that the reaction time (including successive filtrations) and consequently the reaction conversion was affected by two factors of viscosity and polarity of the used solvents. In order to use all the surface of the filter paper (covering the whole surface of the paper with the reaction mixture), the amount of solvent for all reactions was 5 mL and also molecular oxygen (bubbling in the reaction mixture) was used as an oxidant. Table S9 shows the effect of a wide range of solvents with different polarity and viscosity on the benzyl alcohol oxidation. Note to protic nature of benzyl alcohol, protic solvents along with benzyl alcohol can diffuse into the filter paper by H-bonding. On the other hand, due to the presence of polar and protic groups on silica groups and cellulose fibrous in the cellulose filter paper, this interaction resulted in better contact between the reactants and the filter paper surface. As shown in Table S9, the highest efficiency occurs in acetic acid and H₂O: EtOH mixture (Table S9, entries 1,5). Contrary to the effect of oxidant type, solvent type did not show a significant effect on selectivity towards benzaldehyde, and for all solvents tested, benzaldehyde was the major product. Aprotic solvents such as CH₃CN (Table S9, entry 2), THF (Table S9, entry 6), and DMSO (Table S9, entry 9) didn't give any significant conversion. Ethanol provided low conversion for benzaldehyde (Table S9, Entry

4). It seems that the addition of water to the reaction mixture causes better diffusion and contact of the reactants in the filter paper and consequently stronger interaction with the catalytic active sites. The reaction time increased in high viscosity solvents such as DMSO (2 cp) and give lower conversion than H₂O: EtOH solvent.

Temperature did not have a positive effect on the %conversion of benzyl alcohols, except that at temperatures above 50 °C (water bath temperature), selectivity decreased. As shown in Table S10, oxidation at room temperature has the highest efficiency and remains constant as the temperature rises to the boiling point of solvent.

Thus, the oxidation of benzyl alcohols was performed by filtration method using catalytic filter paper (containing 2 mmol Mn/95 cm²) in the presence of molecular oxygen and at room temperature. Also, the direct oxidation of alcohol to carboxylic acid was performed under the same conditions, except that NaOCl was used as the oxidant instead of molecular oxygen. In order to prepare Schiff base and oxime compounds, conditions similar to the oxidation of alcohols to aldehydes in the presence of amines and hydroxylamine hydrochloride were used respectively.

3.4. Catalytic studies over the FP@Si-Mn^{III}-Salen-TEMPO

In following, the catalytic activity of the filter paper was studied to oxidize a wide range of benzyl alcohols. Table 1 shows the results of these studies on a wide range of benzyl alcohols and a few secondary alcohols. As shown in Table 1, the oxidation of benzyl alcohols to aldehyde and carboxylic acid was performed in the presence of molecular O₂ and NaOCl, respectively. Good to excellent conversion was obtained for most derivatives. The efficiency for benzyl alcohols with electron donor substituents was better than those containing electron withdrawing group. In the case of products with low melting points and solubility such as **9f**, **9g**, **9i**, it caused the products to remain on the catalytic filter paper and facilitated the separation and workup stages. The lower reactivity of the secondary alcohols increased the filtration cycles, so that for **9m** and **9o** (6 consecutive filtrations) 80 and 65% conversion were achieved, respectively for 100 min. No detectable efficiency was observed for the oxidation of cyclohexanol (Table 1, entry 14). The selectivity for direct oxidation of alcohols to carboxylic acids was lower than their conversion to aldehydes and was found as %94 (on average).

Then, the catalytic activity of the filter paper to prepare imines and oximes using the corresponding alcohols was studied. At first, it seemed that the deposition of oximes and Schiff bases in the first and second filtration caused a decrease in efficiency in the next cycles and incompleteness of the reaction, but according to the results, most of the reactions have reached to completion. This phenomenon can be directly attributed to the influence of effective diffusion of reactants and constant amount of effective concentration of the reactants. As shown in Tables 2 and 3, good to excellent efficiencies were obtained for all derivatives.

3.5. Control experiments

In order to clarify that the catalytic properties of FP@Si-Mn^{III}-Salen-TEMPO is unique, the catalytic activity of differ-

ent types of filter papers and different salts and compounds were studied and compared over the aerobic oxidation of benzyl alcohol. The effect of the presence of TEMPO groups on oxygen transfer was determined by examining the catalytic activity of Mn^{III}-Salen complex **4**. As shown in Table 4, Mn^{III}-salen complex **4** gave only 36% conversion for 37 min (Table 4, Entry 1). In addition, the selectivity was significantly reduced (66%). Also, immobilization of this complex on the cellulose filter paper did not have a significant effect on the efficiency and selectivity (Table 4, entry 2). Interestingly, Mn^{III}-salen-TEMPO gave less activity than when immobilized on the filter paper. Mn^{III}-salen-TEMPO gave 90% conversion for 37 min (under homogeneous conditions) and 98% for 120 min. However, the selectivity remained constant at 95% until the end of the reaction, which was lower than the observed selectivity for FP@Si-Mn^{III}-Salen-TEMPO (above 97%). Despite the homogeneous catalytic activity of the Mn^{III}-salen-TEMPO, the superiority of filter paper **7** over Mn^{III}-salen-TEMPO can be attributed to its immobilization between the cellulose chains and the set-up mode, which respectively causes stereochemistry control (proper contact between reactants and the active sites in the cellulose fibrous, which causes high selectivity) and effective concentration, to processed the oxidation even at low concentrations.

FP@salen-TEMPO filter paper (ligand) also provided conversion as same as Mn(OAc)₂·4H₂O (Table 4, entry), reflecting the simultaneous catalytic effect of the coordinated Mn and TEMPO groups on the salen framework, acting as an immobilized bi-functional catalyst on the cellulose filter paper.

Finally, based on control experiments results, the effect of TEMPO groups on product selectivity was clarified (Table 4, entries 6 and 7). Initially, a physical mixture of 4 mmol TEMPO with 2 mmol of Mn^{III}-Salen complex **4**, gave only 88% conversion with a low selectivity of 60%. In the second test, the presence of TEMPO free groups on FP@Mn^{III}-Salen filter paper gave 92% and %88 conversion and selectivity, respectively.

Immobilization of TEMPO groups on the catalyst surface was an intelligent strategy that causes to their stability on

the heterogeneous catalyst as well as possibility of recovery in order to be cost-effective and environmentally friendly. However, in this study, (as well as previously published reports (Ma, et al., 2019; Chandra, Jonas, & Fernandes, 2018) showed that the immobilization of TEMPO groups on the catalyst surface has different and significant effects than when it was used as a free reagent in the reaction mixture, so that not only increases the reaction efficiency, but also controls the selectivity of the reaction.

The results of control experiments well showed that the components including Mn^{III}-salen complex, the presence of TEMPO moieties, immobilized on cellulose fibrous were highly correlated with each other, so that the removal of each of them led to the loss of catalytic activity. The results also showed that the free-TEMPO filter paper (FP@Mn^{III}-Salen, Table 4, entry 2) gave lower selectivity than when it was immobilized on the filter paper (in the salen structure). As will be shown in the proposed mechanism, the bi-functional structure of the catalyst causes the alcohol substrate to be fixed between the TEMPO and the Mn centers, provides high selectivity in agreement with the literature (Dijksman, Arends, & Sheldon, 2003; Ma, et al., 2019; Mahmoudi, Rostami, Kazemnejadi, & Hamah-Ameen, 2020).

In other two control experiments, direct oxidation of benzyl alcohol to benzoic acid in the presence of NaOCl and aniline (as well as NH₂OH·HCl) was performed over FP@Si-Mn^{III}-Salen-TEMPO catalytic filter paper. The results did not show any products for benzaldehyde oxime or *N*,1-diphenylmethanimine (Scheme S2). Therefore, the catalytic filter paper has a high chemoselectivity towards the oxidation of alcohol to benzoic acid than the direct conversion to imine or oxime, two reactions that also have low activation energy (Khalaji, et al., 2017). The conversion and selectivity of benzoic acid were 97% and 94%, respectively (exactly the same as before), which reflects the non-interference of aniline or NH₂OH in the direct oxidation of alcohol to benzoic acid.

In order to achieve the best performance of the filter paper, how to apply it in the reaction was studied in 3 different sets ups (Scheme 3), including (1) cutting the filter paper and using

Table 4 Control experiments in the presence of some reagents as well as homologues of the filter paper **7** over the aerobic oxidation of benzyl alcohol^a.

| Entry | Filter paper type/ Mn complex | Time (min) | Conversion (%) | Selectivity (%) |
|-------|--|------------|-----------------|-----------------|
| 1 | Mn ^{III} -Salen complex 4 ^b | 37 | 36 | 66 |
| 2 | FP@Mn ^{III} -Salen ^c | 37 | 30 | 70 |
| 3 | Mn ^{III} -salen-TEMPO ^b | 37 | 90 ^d | 95 |
| 4 | Mn(OAc) ₂ ·4H ₂ O ^b | 37 | 20 | 30 |
| 5 | Plain filter paper ^c | 37 | N.R. | – |
| 6 | FP@salen-TEMPO ligand ^c | 37 | 20 | 25 |
| 7 | Mn ^{III} -Salen complex 4 + TEMPO ^c | 37 | 88 | 60 |
| 8 | FP@Mn ^{III} -Salen + TEMPO (4.0 mmol) | 37 | 92 | 88 |

^a Overall reaction conditions: Benzyl alcohol (1.0 mmol), EtOH: H₂O (2:1, v/v, 5.0 mL), O₂ bubbling (1.0 mL min).

^b 2.0 mmol.

^c The reactions using filter papers (entries 4–6) were performed at room temperature with 1 mL/min O₂ inlet bubbling. Other reactions were performed in a 10 mL round bottom balloon stirred with magnetic stirrer bar equipped with 1 mL/min O₂ inlet bubbling. Loading of Mn (mmol/95 cm²) was about 2.0 ± 0.2.

^d 98% conversion for 120 min.

^e A physical mixture of Mn^{III}-salen complex **4** (2.0 mmol) and TEMPO (4.0 mmol) was added to the mixture.

it in the reaction mixture (like a heterogeneous catalyst), (2) suspending the filter paper components inside the reaction mixture, and (3) filtration mode equipped with a O₂ flow (instead of O₂ bubbling). Reactions were compared to prepare **9a**, **10a**, and **12a**. Although, set ups of 1 and 2 gave moderate to high efficiency for the compounds (with similar selectivity to the filtration mode), their efficiency was significantly different from the filtration mode. In addition, the amount of shrinkage and swellability in these methods was more and less than the filtration method, respectively.

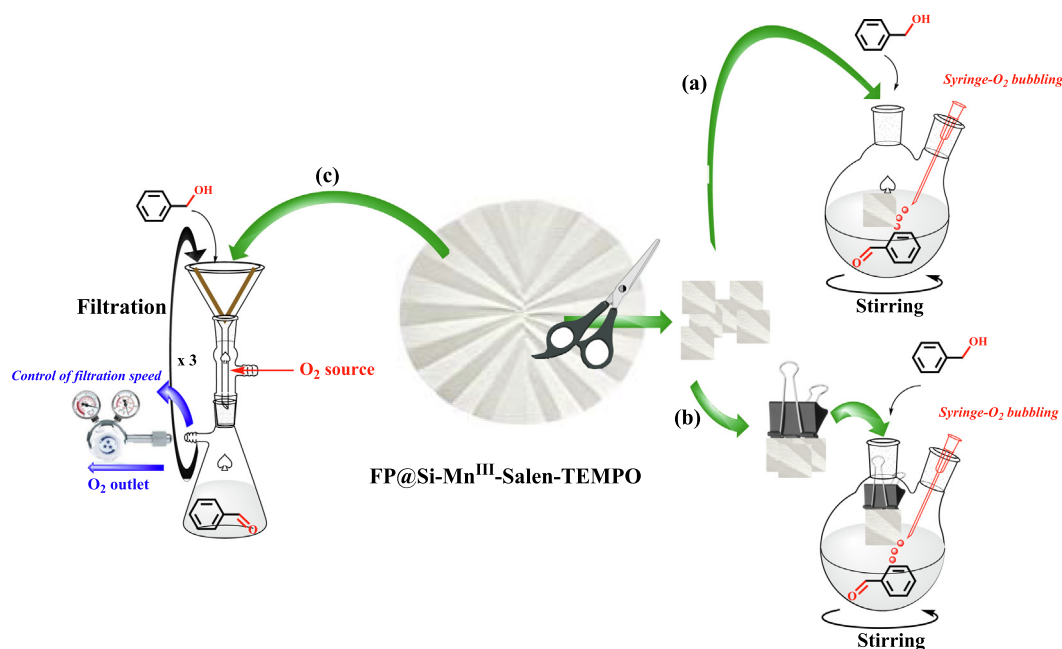
As shown in Table S11, the efficiency for the suspended mode was also lower than the case when using pieces of the filter paper in solution. In contrast, the set up reaction with O₂ gas flow showed almost the same performance as the filtration method. This method was also proposed as a method for performing filtration reactions under a specific gas atmosphere, but in this paper, in order to facilitate successive filtrations, molecular oxygen bubbling was performed with a syringe.

3.6. Mechanism studies

To investigate the effect of the presence of Mn active sites in the immobilized salen complex on the filter paper, the Mn centers were poisoned with an excess amount of mercury (0) (Min, et al., 2021). For this purpose, the catalytic filter paper in ethanolic solution of metallic mercury (0) (240 mmol) was shaken in a petri dish for 2 h and then used in the benzyl alcohol oxidation to benzaldehyde in the presence of molecular oxygen after complete drying. The results did not show any catalytic activity for 37 min (three consecutive filtrations) on the filter paper. Considering that the presence of TEMPO groups in the filter paper under O₂ have oxidizing activity (refer to control experiments), it can be concluded that mercury causes poisoning of both Mn and TEMPO sites. Therefore, according to the results, both Mn and TEMPO active sites have simultane-

ous oxidation activity and are correlated, so that the removal of each component, reduces the catalytic activity.

In order to elucidate the effect of TEMPO moieties in FP@Si-Mn^{III}-Salen-TEMPO on the oxidation of alcohols, the TEMPO moieties were selectively blocked by hydroquinone (Bendary, Francis, Ali, Sarwat, & El Hady, 2013; Chen, Hack, Iyer, Jones, & Opila, 2017; Fónagy, Szabó-Bárdos, & Horváth, 2021). FP@Si-Mn^{III}-Salen-TEMPO catalytic filter paper was treated with an excess amount of hydroquinone. Hydroquinone inactivates TEMPO moieties, rendering them to inactive TEMO-H groups, while having no effect on the Mn centers. An excess amount of hydroquinone (200 mmol) was used to ensure that all TEMPO centers were blocked by hydroquinone. The study of benzyl alcohol oxidation by the filtration method under these conditions produced similar results to the performance of FP@Mn^{III}-Salen (Table 4, entry 2). According to the results, the %conversion and %selectivity were found to be 36 and 72%, respectively. Of note was the high selectivity observed for benzaldehyde relative to the FP@salen-TEMPO ligand, indicating the effect of Mn centers. Therefore, due to the low selectivity in the absence of Mn centers in the FP@salen-TEMPO ligand as well as the results of control experiments (Table 4), it can be concluded that Mn centers are active centers and TEMPO groups play an oxygen transfer role (a co-oxidant agent). The results are completely in line with the results reported by Mahmoudi *et al.* (Mahmoudi, Rostami, Kazemnejadi, & Hamah-Ameen, 2020) of the bi-functional catalyst, including the Co^{III} and TEMPO centers. Based on the results of optimization experiments under air atmosphere (Table S8), it was shown that the oxidation of benzyl alcohol was strongly dependent on the presence of molecular oxygen. Therefore, based on the observations in this study and the previously reported results on bi-functional catalysts including TEMPO and coordinated transition metal, two mechanisms for the oxidation of benzyl alcohols to aldehydes and



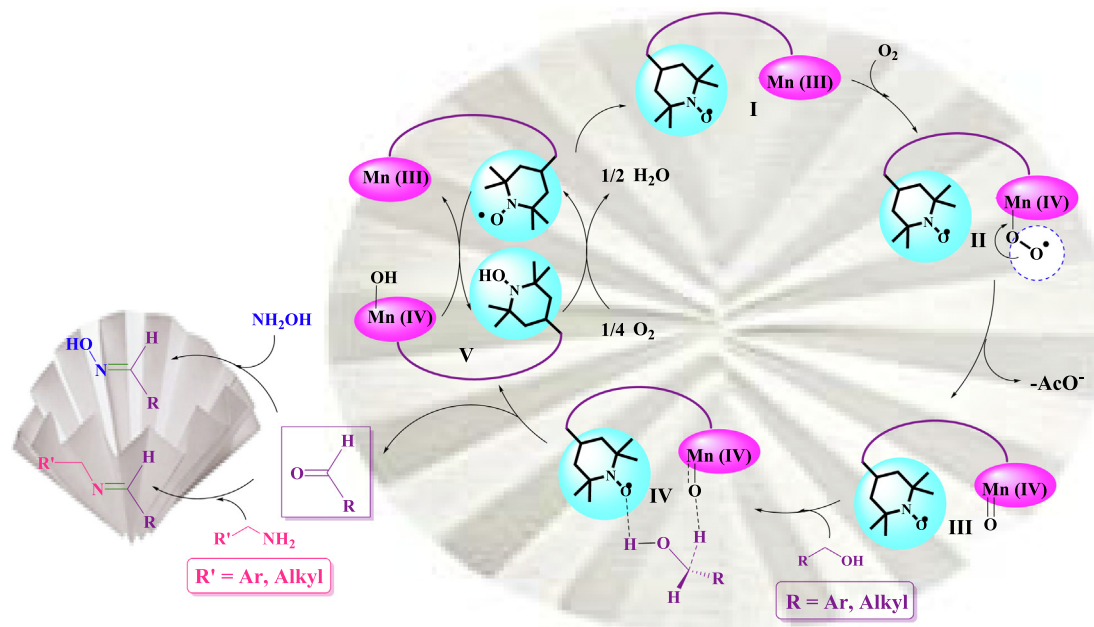
Scheme 3 Examination of three different set-ups for FP@Si-Mn^{III}-Salen-TEMPO oxidation of benzyl alcohol to benzaldehyde.

carboxylic acids were proposed (Scheme 4). Schemes 4 and S2 show two proposed mechanisms for (1) the oxidation of benzyl alcohols to aldehydes, and the subsequent formation of imine and oxime, as well as (2) the direct oxidation of alcohol to acid in the presence of NaOCl respectively. As shown in Scheme S3, the dissolution of molecular oxygen in the solvent causes binding to Mn centers followed by their oxidation (formation of intermediate II) (Kazemnejadi, Shakeri, Mohammadi, Tabefam, 2017). Previously, Mahmoudi *et al.* (Mahmoudi, Rostami, Kazemnejadi, & Hamah-Ameen, 2020; Mahmoudi, Rostami, Kazemnejadi, & Hamah-Ameen, 2021), showed that oxygen in the presence of a bi-functional catalyst bearing TEMPO groups and Co-Schiff base complex, causes oxidation of the Co centers followed by oxidation of the organic compound. Next, by removing an ^-OAc ligand, the $Mn = O$ (III) intermediate is formed. The alcohol diffuses to the filter paper and was linked to the active catalytic centers through OH and H(1) groups by TEMPO and $Mn = O$ groups, respectively (Kazemnejadi, Nikookar, Mohammadi, Shakeri, & Esmailpour, 2018). Due to the fact the bi-functional nature of the active sites, this linkage creates a synergistic effect on the selective oxidation of alcohol to aldehydes on the catalyst surface. Then, in the presence of amine groups (including aryl amines or $NH_2OH \cdot HCl$) in the reaction mixture, the oxime or imine products are formed on the surface of the catalyst. Separation of imine (or oxime) products from the surface of the catalyst causes the reaction to proceed forward and the effective concentration on the surface of the catalyst to oxidize benzyl alcohol remains constant (according to Le Chatelier's principle). In the next step, the presence of molecular oxygen as well as TEMPO groups causes the catalyst to return to its original state (intermediate V), and the catalyst returns to the cycle

(Nutting, Rafiee, & Stahl, 2018; Hu, & Kerton, 2012; Ma, et al., 2019; Cheng, Wang, Wang, & Wu, 2010).

As shown in the proposed mechanism (Scheme 4), the bi-functional structure of the catalyst causes the alcohol substrate to be fixed between the TEMPO and the Mn centers, causing the oxygen transfer and the oxidation to be controlled and prevents further oxidation to acid (or the formation of various oxidation products). But the presence of each component (TEMPO or Mn sites) alone changes the conditions for the fate of oxidation. This is an advantage of the bi-functional catalysts over single-component catalysts (in most cases, of course) as the most acceptable mechanism for the bi-functional systems (Dijksman, Arends, & Sheldon, 2003; Ma, et al., 2019; Mahmoudi, Rostami, Kazemnejadi, & Hamah-Ameen, 2020).

Due to the fact that the presence of NaOCl causes direct oxidation of benzyl alcohols to carboxylic acid, a different mechanism was proposed for it. Such behavior with change of oxidant has also been previously reported for such bi-functional catalysts (Mahmoudi, Rostami, Kazemnejadi, & Hamah-Ameen, 2020; Mahmoudi, Rostami, Kazemnejadi, & Hamah-Ameen, 2021). Unlike molecular oxygen, NaOCl oxidizes TEMPO groups and converts them to peridinium chloride intermediate (Scheme S3, intermediate II) (Ma, et al., 2019; Chandra, Jonas, & Fernandes, 2018; Sharma, Buckley, & Asefa, 2008; Lu, et al., 2008). Diffused alcohols to the catalytic filter paper were adsorbed on the active centers (TEMPO as well as Mn active sites) and form intermediate III, which leads to the formation of the aldehyde product. According to the results of control experiments, where no imine or oxime product was observed in the presence of aniline or $NH_2OH \cdot HCl$, this step seems to be very fast, and is there-



Scheme 4 A plausible reaction mechanism for the aerobic oxidation of benzyl alcohol to carbonyl compounds and its subsequent transformation to oxime (in the presence of $NH_2OH \cdot HCl$) and imine (in the presence of amine) catalyzed by FP@Si-Mn^{III}-Salen-TEMPO catalytic filter paper.

fore shown as an intermediate (Scheme S3). Coordination of aldehydes to Mn(III) centers through the carbonyl group provides the conditions for rapid nucleophilic attack by water (intermediate IV), and by the separation of another proton from C1 (by ⁻OCl), the carboxylic acid product is formed. The nucleophilic attack probably occurs immediately after aldehyde formation. Finally, by the effect of NaOCl groups, the filter paper is returned to its original state and the catalytic cycle is repeated.

3.7. Reusability studies of FP@Si-Mn^{III}-Salen-TEMPO filter paper

In the next section, recoverability as one of the advantages of the filter paper, was studied. Due to the fact that filter paper must be used frequently, its recoverability while maintaining its catalytic properties is of great importance. For this purpose, the catalyst recovery during 4 consecutive cycles in reactions of (1) oxidation of benzyl alcohol to benzaldehyde in the presence of molecular oxygen and (2) direct oxidation of benzyl alcohol to benzoic acid in the presence of NaOCl was investigated. At the end of each cycle, the %conversion and %selectivity towards the desired product was recorded and then the catalyst was reused after washing and drying. As shown in Table S12, no decrease in benzyl alcohol conversion as well as in selectivity for oxidation to benzaldehyde was observed in the presence of molecular oxygen during 4 consecutive cycles, reflecting stability of the filter paper during successive wetting–drying cycles. But in the reaction of direct oxidation of benzyl alcohol to benzoic acid, although the %conversion did not decrease significantly (which was completely consistent with leaching studies in the presence of NaOCl, that will be shown in the next section), but the %selectivity after the fourth cycle decreased to 86%. Due to the lack of significant leaching of Mn metal in successive cycles, the decrease in selectivity can be attributed to the possible oxidation of hydroxyl groups in the cellulose fibrous and their consequent effect on the interaction between the reactant and the catalytic active centers. The characteristic properties associated with cellulose fibers such as insolubility in many solvents and the rigidity of the chain, are related to their hydroxyl groups that forms both intra- and intermolecular hydrogen bonds (Wei, et al., 2018). According to a study by Coseri *et al.*, the presence of NaOCl along with TEMPO groups causes the oxidation of benzyl alcohol groups in cellulose (Coseri, et al., 2015). Therefore, it is also possible that the oxidation of benzylic substituents in cellulose under these conditions causes a change in the possible interactions, and consequently a decrease in the selectivity.

Preservation of the catalytic activity of FP@Si-Mn^{III}-Salen-TEMPO owes to the lack of leaching of Mn into the reaction mixture, which was due to the covalent immobilization of the Mn-salen complex to the cellulose fibrous. During recycling studies (Table S12), in each reaction (after completion of the reaction), the remaining solution was studied by ICP-MS analysis to measure the leaching of Si and Mn metals. The analyzes did not show any trace of Si and Mn metals until the end of the fourth cycle, which reflects the absence of any metal leaching in solution. In fact, the catalyst was designed in such a way that it does not create any soluble part due to the contact and successive passage (filtration) of solvents, and this issue, along with the stable coordination of Mn to

the ligand framework, has caused no metal leaching from the filter paper. Therefore, the slight decrease in efficiency can be attributed to the decrease in the filter paper quality in successive wetting–drying cycles. As will be shown below, during successive wetting–drying cycles, the plain paper undergoes some shrinkage and reduced swellability.

In addition, the hot filtration test was also studied on the oxidative catalytic filter paper. For this purpose, in the model benzyl alcohol oxidation, after the second filtration (75% conversion, 12 min), the filtration was stopped and the filter paper was removed (Scheme S4). Then, a magnet was added to the collected reaction mixture (residue) and stirred at room temperature for 1 h. After this time, the %conversion reached to 77% (GC analysis). The results showed well that despite successive filtrations, the Mn leaching was insignificant due to the coordination to a stable salen ligand. The results of EDX and leaching were completely consistent with these results and confirm the stability, lack of contamination and reproducibility of the modified filter paper.

In following, the oxidative filter paper was characterized by EDX and FE-SEM analyses after 4th cycle in the oxidation of benzyl alcohol to benzaldehyde in the presence of molecular oxygen. This analysis was performed to ensure the adsorption of any impurities (including raw materials and products) on the filter paper after repeated use. As shown in Figure S15a, the %wt of C, O, N, Mn elements has not changed significantly, which reflects the filtration and subsequent complete washing of the filter paper after filtration. In addition, this analysis showed that the absence of any impurities in the filter paper after the reaction not only does not cause a loss of efficiency, but also allows its repeated use with confidence. In addition, the FE-SEM image of the recovered filter paper (Figure S15b) showed that its morphology did not change compared to the freshly prepared filter paper, which reflects the high stability and immobilization of the Mn complex through strong covalent bonding.

The stability of the filter paper and subsequently the immobilized compounds was studied in various acidic, alkaline, and oxidative solutions. In this study, the solutions prepared from NaOCl, HNO₃, HCl, NaOH and H₂O₂ were filtered ten times by the catalytic filter paper 7 and then the filter paper obtained by EDX and the following residue were analyzed by ICP to check the leaching of Mn. Table S13 summarizes these results for both filter paper and the corresponding residue. According to the results, the filter paper showed very good stability in alkaline and oxidative media. No leaching due to Mn and Si metals was observed due to filtration of NaOCl, NaOH 0.1 N, and 37% H₂O₂ (Table S13, entries 1, 4, 5). EDX analysis of the filter paper also confirmed these results and no significant change in the elemental composition of the filter paper was observed (Table S13, entries 6, 9, 10). The stability of the iminium bond (in the Mn-salen complex) and its immobilization through covalent bonding has caused considerable stability for the filter paper in alkaline and oxidative media, thus making it very suitable for use in these media. In this study, the filter paper was also successfully used in a completely oxidizing media. The filter paper underwent leaching in acidic media (Table S13, entries 2,3). As shown in Table S13, filtration of 0.1 N HNO₃ results in significant leaching of Mn and Si. Leaching values were much lower for 0.1 N HCl, and was equal to 1.12 %wt and 0.11 %wt for Mn and Si, respectively, while for HNO₃ they were 4.56 %wt and 6.32 %wt,

respectively. The results of EDX from the treated filter paper with these acids also confirmed the results (Table S13, entries 8, 9). Imine bond, and also ether bond hydrolysis (the linkage between cellulose fibrous and the Mn-salen complex) on the filter paper in acidic media was the main cause of Si and Mn leaching from filter paper.

Next, the effect of different pHs on the catalytic filter paper was studied. For this purpose, using HCl and NaOH solutions, the filter paper leaching was measured at pHs in the range of 1–14. The results were shown in terms of %wt Mn leached from the filter paper (Figure S16). In each reaction, 5 mL of each prepared pH was filtered 10 times and then the reaction mixture was studied by ICP-MS analysis towards Mn leaching. According to the results, with decreasing pH from 4 to 1, the amount of leaching Mn increases linearly, so that the amount of leaching at pH = 4 was equal to 2% wt and at pH = 1 almost complete leaching occurs. On the other hand, significant stability was observed at high pHs for the filter paper, which at pH = 14 only 1.4% wt Mn leaching was observed in the residue. Although the hydrolysis of the iminium bond also takes place in the basic media (Kazemnejadi, Rezazadeh, Nasseri, Allahresani, & Esmacilpour, 2019), the results show that this bond was more stable under basic conditions; In addition, the etheric bond linkage (the linkage between cellulose fibrous and the Mn-salen complex) does not undergo hydrolysis at high pHs, and is one of the factors of low leaching of these metals at alkaline pHs. It is noteworthy that at pHs 5–11 no leaching were detected for Mn and Si metals, which reflects the remarkable stability of the groups immobilized by covalent bonding on the filter paper.

The swellability of the filter paper is one of the important parameters that affects the catalytic activity of the filter paper (Sahin, & Arslan, 2008). Due to the continuous wetting–drying in the filter paper, the catalyst recovery capability was highly dependent on the degree of swellability. For this purpose, the swelling rate of the filter paper during successive cycles in EtOH: H₂O (2: 1) as well as NaOCl/ EtOH: H₂O was studied. Chemical modifications on cellulosic fibrous have been shown to affect their %swelling (Wistara, & Young, 1999; Weise, & Paulapuro, 1996). At each stage, the filter paper was dried for 12 h at 35 °C in a vacuum oven and then used. Figure S17 shows the results of the swelling and shrinkage for both EtOH: H₂O (2: 1) and NaOCl/ EtOH: H₂O solutions, where the swellability for these two solutions decreased from 15.0 and 14.4 to 13.8 respectively for 5 consecutive wetting–drying cycles. This insignificant reduction in swellability could be due to the presence of silica linkers in the cellulose structure, which can act as a cross-linker between cellulose fibrous, and promotes its swellability. These results were completely consistent with the thermal behavior of the silylated filter paper (Figure S17-b). Assuming that the CPTES group was attached to cellulose only through one of the methoxy groups, the other two groups have the potential to interact and subsequently crosslink between the cellulose fibrous. This was also one of the reasons for the high swelling amount observed for solvents after silylation (Figure S17). Therefore, this slight decrease in the swelling could also be due to a change in the amount of crosslinking between the chains due to a change in the fibrous structure of the polymer during successive wetting–drying. Another factor was the closure of larger porosities during re-wetting, which are unable to reopen and can cause surface tension forces (Sahin, & Arslan, 2008). The

Schiff base bonds on the surface of the filter paper, along with the silica cross-links, greatly reduce the shrinkage of the filter paper and minimize the closure of the porosities, which are the main barrier to solvent diffusion. The results were completely consistent with the previously published reports on the swellability of cellulose paper after drying (Wistara, & Young, 1999). However, the slight decrease in leaching has also been responsible for the slight decrease in alcohol oxidation efficiency. Re-measuring the diameter of the filter paper showed no significant shrinkage (diameter reduction of 1 mm) and the diameter of the filter paper after 5 consecutive wetting–drying cycles was 5.4 and 5.0 cm for EtOH: H₂O (2: 1) as well as NaOCl/ EtOH: H₂O solutions.

In order to ensure the effect of the presence of Schiff base groups (in the Mn^{III}-salen complex) as well as silica groups in cellulose fibrous in reducing shrinkage and swelling after successive wetting–drying, in a separate analysis, plain and silylated filter paper were also subjected to successive wetting and drying in EtOH: H₂O solvent and their swelling rate was measured at each stage. In accordance with the published articles, the plain filter paper undergoes a lot of shrinkage at each stage, so that at the end of successive wetting–drying cycles (5 consecutive cycles), the paper undergoes about 7 mm decrease in diameter, and swelling rate of 13.3 mL/g reaches to 8.6 mL/g. But for the silylated filter paper, the amount of shrinkage was equal to 2 mm and the amount of swelling reduced to 12 mL/g, which was insignificant. Surface silylation stops the shrinkage and subsequently preserves swelling by creating a possible crosslinking (ESI, Fig. S18).

4. Conclusion

A plain and cheap cellulose filter paper was transformed to a valuable sustainable catalytic filter paper by some modifications including silylation followed by Mn(III)-salen complex immobilization. The modified filter paper was applied towards switchable-selective oxidation of benzyl alcohols to aldehyde and carboxylic acid in the presence of molecular O₂ and NaOCl oxidant respectively. In addition, direct conversion of alcohol to imine as well as oxime was performed on this filter paper in the presence of amine and NH₂OH·HCl in one step, respectively. The high selectivity of the bi-functional filter paper resulted in high selectivity for carbonyl and carboxylic acid products, without any by-products. Extensive studies on control experiments have shown that TEMPO and Mn-salen complex have a high correlation and significant synergistic effect for the oxidation of organic compounds, so that the removal of either component in the paper causes a significant decrease in the reaction efficiency. Recovery studies on the filter paper showed high stability with minimal leaching and shrinkage due to its modifications with silica and iminium bonds. The filter paper also has high stability in oxidative and alkaline media and a relative stability in acidic media. High stability in acidic and basic pHs, reusability and recyclability with minimal shrinkage and metal leaching, preservation of catalytic activity during several consecutive wetting–drying, easy work-up, mild reaction conditions, etc. are some of the advantages of the present novel protocol, which makes it as a promising alternative catalytic system for environmentally friendly reactions. However, the flirtation mode of the present study, limits its application in continuous flow reactions. On the other hand, the designed modified-cellulose filter paper can also be used as a reliable platform for solid phase synthesis reactions as well as three-phase tests to study heterogeneous nature of the catalysts. By changing the inlet gas, the type of reaction can be changed; For example, reduction reac-

tions (with ex situ generated H₂ gas) and carbonization (with CO₂ gas), which are currently being performed in our laboratory by various modifications on the filter paper.

Declaration of Competing Interest

The authors declare that they have no known competing financial interests or personal relationships that could have appeared to influence the work reported in this paper.

Acknowledgements

The authors gratefully acknowledge the financial support provided by Talent introduction project of Guangdong university of petrochemical technology(2018rc50), Open fund of Guangdong provincial key laboratory of petrochemical pollution process and control, Guangdong university of petrochemical technology (No. 2018B030322017), Science and technology plan project of Maoming city (2019395).

Appendix A. Supplementary material

FTIR & NMR characterization of 1-4 compounds, design expert data, and some characterization study of the filter paper 7 are available in supplementary file. Supplementary data to this article can be found online at <https://doi.org/10.1016/j.arabjc.2022.104140>.

References

- Baran, N.Y., Saçak, M., 2017. Synthesis, characterization and molecular weight monitoring of a novel Schiff base polymer containing phenol group: thermal stability, conductivity and antimicrobial properties. *J. Mol. Struct.* 1146, 104–112.
- Bendary, E., Francis, R.R., Ali, H.M.G., Sarwat, M.I., El Hady, S., 2013. Antioxidant and structure–activity relationships (SARs) of some phenolic and anilines compounds. *Ann. Agric. Sci.* 58 (2), 173–181.
- Biesinger, M.C., Payne, B.P., Grosvenor, A.P., Lau, L.W., Gerson, A.R., Smart, R.S.C., 2011. Resolving surface chemical states in XPS analysis of first row transition metals, oxides and hydroxides: Cr, Mn, Fe, Co and Ni. *Appl. Surf. Sci.* 257 (7), 2717–2730.
- Chandra, P., Jonas, A.M., Fernandes, A.E., 2018. Spatial coordination of cooperativity in silica-supported Cu/TEMPO/Imidazole catalytic triad. *ACS Catal.* 8 (7), 6006–6011.
- Chantreau, G., Brown, N., Dourges, M.A., Freire, C.S., Silvestre, A.J., Sebe, G., Coma, V., 2019. Silylation of bacterial cellulose to design membranes with intrinsic anti-bacterial properties. *Carbohydr. Polym.* 220, 71–78.
- Chen, M., Hack, J.H., Iyer, A., Jones, K.J., Opila, R.L., 2017. Radical-driven silicon surface passivation by benzoquinone–and hydroquinone-methanol and photoinitiators. *J. Phys. Chem. C* 121 (39), 21364–21373.
- Cheng, L., Wang, J., Wang, M., Wu, Z., 2010. Mechanistic insight into alcohol oxidation mediated by an efficient green Cu II-bipy catalyst with and without TEMPO by density functional methods. *Dalton Trans.* 39 (22), 5377–5387.
- Coseri, S., Biliuta, G., Zemljčič, L.F., Srndovic, J.S., Larsson, P.T., Strnad, S., Lindström, T., 2015. One-shot carboxylation of microcrystalline cellulose in the presence of nitroxyl radicals and sodium periodate. *RSC Adv.* 5 (104), 85889–85897.
- Deligeorgiev, T., Gadjev, N., Vasilev, A., Kaloyanova, S., Vaquero, J.J., Alvarez-Builla, J., 2010. Green chemistry in organic synthesis. *Mini-Rev. Org. Chem.* 7 (1), 44–53.
- Dijksman, A., Arends, I.W., Sheldon, R.A., 2003. Cu (ii)-nitroxyl radicals as catalytic galactose oxidase mimics. *Org. Biomol. Chem.* 1 (18), 3232–3237.
- Fónagy, O., Szabó-Bárdos, E., Horváth, O., 2021. 1, 4-Benzoquinone and 1, 4-hydroquinone based determination of electron and superoxide radical formed in heterogeneous photocatalytic systems. *J. Photochem. Photobiol. A: Chem.* 407, 113057.
- Fubini, B., Ghiazza, M., Fenoglio, I., 2010. Physico-chemical features of engineered nanoparticles relevant to their toxicity. *Nanotoxicology* 4 (4), 347–363.
- Haider, A., Haider, S., Kang, I.K., Kumar, A., Kummara, M.R., Kamal, T., Han, S.S., 2018. A novel use of cellulose based filter paper containing silver nanoparticles for its potential application as wound dressing agent. *Int. J. Biol. Macromol.* 108, 455–461.
- Hinterstoisser, B., Salmén, L., 2000. Application of dynamic 2D FTIR to cellulose. *Vib. Spectrosc.* 22 (1–2), 111–118.
- Hoover, J.M., Ryland, B.L., Stahl, S.S., 2013. Copper/TEMPO-catalyzed aerobic alcohol oxidation: mechanistic assessment of different catalyst systems. *ACS Catal.* 3 (11), 2599–2605.
- Hospodarova, V., Singovszka, E., Stevulova, N., 2018. Characterization of cellulosic fibers by FTIR spectroscopy for their further implementation to building materials. *Am. J. Anal. Chem.* 9 (6), 303–310.
- Hu, Z., Kerton, F.M., 2012. Simple copper/TEMPO catalyzed aerobic dehydrogenation of benzylic amines and anilines. *Org. Biomol. Chem.* 10 (8), 1618–1624.
- Jankauskaitė, V., Balčiūnaitienė, A., Alexandrova, R., Buškuvienė, N., Žukienė, K., 2020. Effect of cellulose microfiber silylation procedures on the properties and antibacterial activity of polydimethylsiloxane. *Coatings* 10 (6), 567.
- Kamal, T., Khan, S.B., Haider, S., Alghamdi, Y.G., Asiri, A.M., 2017. Thin layer chitosan-coated cellulose filter paper as substrate for immobilization of catalytic cobalt nanoparticles. *Int. J. Biol. Macromol.* 104, 56–62.
- Kazemnejadi, M., Shakeri, A., Mohammadi, M., Tabefam, M., 2017. Direct preparation of oximes and Schiff bases by oxidation of primary benzylic or allylic alcohols in the presence of primary amines using Mn(III) complex of polysalicylaldehyde as an efficient and selective heterogeneous catalyst by molecular oxygen. *J. Iran. Chem. Soc.* 14 (9), 1917–1933.
- Kazemnejadi, M., Nikoogar, M., Mohammadi, M., Shakeri, A., Esmailpour, M., 2018. Melamine-Schiff base/manganese complex with dendritic structure: an efficient catalyst for oxidation of alcohols and one-pot synthesis of nitriles. *J. Colloid Interface Sci.* 527, 298–314.
- Kazemnejadi, M., Rezazadeh, Z., Nasseri, M.A., Allahresani, A., Esmailpour, M., 2019. Imidazolium chloride-Co(III) complex immobilized on Fe₃O₄@SiO₂ as a highly active bifunctional nanocatalyst for the copper-, phosphine-, and base-free Heck and Sonogashira reactions. *Green Chem.* 21 (7), 1718–1734.
- Khalaji, A.D., Mighani, H., Kazemnejadi, M., Gotoh, K., Ishida, H., Fejfarova, K., Dusek, M., 2017. Synthesis, characterization, crystal structure and theoretical studies on 4-bromo-2-[(E)-6-methyl-2-pyridyliminomethyl] phenol. *Arabian J. Chem.* 10, S1808–S1813.
- Koga, H., Kitaoka, T., Isogai, A., 2012. Immobilized enzyme as a green microstructured catalyst. *J. Mater. Chem.* 22 (23), 11591–11597.
- Li, Q., Wang, S., Jin, X., Huang, C., Xiang, Z., 2020. The application of polysaccharides and their derivatives in pigment, barrier, and functional paper coatings. *Polymers* 12 (8), 1837.
- Lin, N., Huang, J., Dufresne, A., 2012. Preparation, properties and applications of polysaccharide nanocrystals in advanced functional nanomaterials: a review. *Nanoscale* 4 (11), 3274–3294.
- Lu, Z., Costa, J.S., Roubeau, O., Mutikainen, I., Turpeinen, U., Teat, S.J., Reedijk, J., 2008. A copper complex bearing a TEMPO moiety as catalyst for the aerobic oxidation of primary alcohols. *Dalton Trans.* 27, 3567–3573.

- Ma, Z., Wang, Q., Alegria, C.B.A., E., C Guedes da Silva, M. F., MDRS Martins, L., Telo, J. P., & JL Pombeiro, A., 2019. Synthesis and structure of copper complexes of a N_6O_4 macrocyclic ligand and catalytic application in alcohol oxidation. *Catalysts* 9 (5), 424.
- Ma, Z., Mahmudov, K.T., Aliyeva, V.A., Gurbanov, A.V., Pombeiro, A.J., 2020. TEMPO in metal complex catalysis. *Coord. Chem. Rev.* 423, 213482.
- Mahmoudi, B., Rostami, A., Kazemnejadi, M., Hamah-Ameen, B.A., 2020. Catalytic oxidation of alcohols and alkyl benzenes to carbonyls using $Fe_3O_4@SiO_2@(TEMPO)\text{-co}\text{-}(Chlorophyll\text{-}Co^{III})$ as a bi-functional, self-co-oxidant nanocatalyst. *Green Chem.* 22 (19), 6600–6613.
- Mahmoudi, B., Rostami, A., Kazemnejadi, M., Hamah-Ameen, B.A., 2021. Oxidation/MCR domino protocol for direct transformation of methyl benzene, alcohol, and nitro compounds to the corresponding tetrazole using a three-functional redox catalytic system bearing TEMPO/Co (III)-porphyrin/Ni (II) complex. *Mol. Catal.* 499, 111311.
- Min, Q., Miao, P., Chu, D., Liu, J., Qi, M., Kazemnejadi, M., 2021. Introduction of a recyclable basic ionic solvent with bis-(NHC) ligand property and the possibility of immobilization on magnetite for ligand-and base-free Pd-Catalyzed Heck, Suzuki and Sonogashira cross-coupling reactions in water. *Catal. Lett.*, 1–18
- Mourya, M., Choudhary, D., Basak, A.K., Tripathi, C.S.P., Guin, D., 2018. Ag-nanoparticles-embedded filter paper: an efficient dip catalyst for aromatic nitrophenol reduction, intramolecular cascade reaction, and methyl orange degradation. *ChemistrySelect* 3 (10), 2882–2887.
- Musikavanhu, B., Hu, Z., Dzapata, R.L., Xu, Y., Christie, P., Guo, D., Li, J., 2019. Facile method for the preparation of superhydrophobic cellulosic paper. *Appl. Surf. Sci.* 496, 143648.
- Niazi, J.H., Gu, M.B., 2009. Toxicity of metallic nanoparticles in microorganisms-a review. *Atmos. Biol. Environ. Monit.*, 193–206
- Nie, S., Guo, H., Lu, Y., Zhuo, J., Mo, J., Wang, Z.L., 2020. Superhydrophobic cellulose paper-based triboelectric nanogenerator for water drop energy harvesting. *Adv. Mater. Technol.* 5 (9), 2000454.
- Nishikata, T., Tsutsumi, H., Gao, L., Kojima, K., Chikama, K., Nagashima, H., 2014. Adhesive catalyst immobilization of palladium nanoparticles on cotton and filter paper: applications to reusable catalysts for sequential catalytic reactions. *Adv. Synth. Catal.* 356 (5), 951–960.
- Nutting, J.E., Rafiee, M., Stahl, S.S., 2018. Tetramethylpiperidine *N*-oxyl (TEMPO), phthalimide *N*-oxyl (PINO), and related *N*-oxyl species: electrochemical properties and their use in electrocatalytic reactions. *Chem. Rev.* 118 (9), 4834–4885.
- Pramanik, K., Sarkar, P., Bhattacharyay, D., 2019. 3-Mercapto-propanoic acid modified cellulose filter paper for quick removal of arsenate from drinking water. *Int. J. Biol. Macromol.* 122, 185–194.
- Sahin, H.T., Arslan, M.B., 2008. A study on physical and chemical properties of cellulose paper immersed in various solvent mixtures. *Int. J. Mol. Sci.* 9 (1), 78–88.
- Sharma, K.K., Buckley, R.P., Asefa, T., 2008. Optimizing acid–base bifunctional mesoporous catalysts for the henry reaction: effects of the surface density and site isolation of functional groups. *Langmuir* 24 (24), 14306–14320.
- Sheibani, E., Hosseini, A., Sobhani Nasab, A., Adib, K., Ganjali, M. R., Pourmortazavi, S.M., Ehrlich, H., 2021. Application of polysaccharide biopolymers as natural adsorbent in sample preparation. *Crit. Rev. Food Sci. Nutr.*, 1–28
- Tang, Q., Jiang, L., Liu, J., Wang, S., Sun, G., 2014. Effect of surface manganese valence of manganese oxides on the activity of the oxygen reduction reaction in alkaline media. *ACS Catal.* 4 (2), 457–463.
- Uhl, F.M., Levchik, G.F., Levchik, S.V., Dick, C., Liggat, J.J., Snape, C.E., Wilkie, C.A., 2001. The thermal stability of cross-linked polymers: methyl methacrylate with divinylbenzene and styrene with dimethacrylates. *Polym. Degrad. Stab.* 71 (2), 317–325.
- Wei, X., Wang, Y., Li, J., Wang, F., Chang, G., Fu, T., Zhou, W., 2018. Effects of temperature on cellulose hydrogen bonds during dissolution in ionic liquid. *Carbohydr. Polym.* 201, 387–391.
- Weise, U., Paulapuro, H., 1996. Relation between fibre shrinkage and hornification. *Papier* 50 (6), 328–333.
- Wistara, N., Young, R.A., 1999. Properties and treatments of pulps from recycled paper. part I. physical and chemical properties of pulps. *Cellulose* 6 (4), 291–324.
- Yao, B., Zhang, J., Kou, T., Song, Y., Liu, T., Li, Y., 2017. Paper-based electrodes for flexible energy storage devices. *Adv. Sci.* 4 (7), 1700107.
- Youssef, A.M., Kamel, S., El-Sakhawy, M., El Samahy, M.A., 2012. Structural and electrical properties of paper–polyaniline composite. *Carbohydr. Polym.* 90 (2), 1003–1007.
- Zhao, Y., Liu, L., Shi, D., Shi, X., Shen, M., 2019. Performing a catalysis reaction on filter paper: development of a metal palladium nanoparticle-based catalyst. *Nanoscale Adv.* 1 (1), 342–346.